The research on p-type formation of AlGaN by Al_4C_3 and the application to light-emitting diodes

September 2014

Kim Dohyung

Contents

CHAPTER 1

INTRODUCTION

1.1 Background

In order to obtain blue light, semiconductor having band-gap energy more than 2.5 eV is needed. However, it is generally difficult to grow the material with wide bandgap. II-VI based binary ZnSe compound with bandgap energy of 2.7 eV has been studied and the productive result was obtained [1-5]. However, the remarkable progress was not achieved. As a result, the commercialization of ZnSe based blue LED got in trouble, compared with red and green LEDs.

AlGaInN-based III nitride semiconductor is wurzite structure and can form continuous alloys with the direct band-gap from 0.65 eV (InN) through 3.4 eV (GaN) to 6.0 eV (AlN) except BN [6, 7]. Especially, the luminous efficiency of red color wavelength (420 nm) was empirically known to be the best [8]. Moreover, the atomic binding energy is bigger than II-VI based material. Hence, it has gathered substantial interest because of the need for highly efficient optoelectronic devices operating in the blue to ultraviolet spectral region.

The method of epitaxy is necessary for growing the crystal of nitride semiconductor. Epitaxy refers to the deposition of a crystalline overlayer on a crystalline substrate, where there is registry between the overlayer and the substrate [9]. Metalorganic Vapor Phase Epitaxy (MOVPE) [10-13], Molecular Beam Epitaxy (MBE) and Hydride Vapor Phase Epitaxy (HVPE) are the applications of epitaxy method. But, growth of III-V based GaN was hard. That reasons are group III and V components has a high melting point and high equilibrium vapor pressure [14]. Furthermore, the absence of the suitable substrate for GaN growth was also problem [15].

Pankove group who firstly reported the GaN growth selected the sapphire having a similar GaN crystal structure as a substrate. But, the differences of lattice constant and therma

l expansion coefficient for GaN and sapphire are 13.8 % and 25.5 % [16]. Difference of lattice constants causes the many dislocations at the interface of GaN and substrate. Actually, the structure of as grown GaN on sapphire substrate was showed the island shape. Also, many dislocations were shown on GaN due to the difference of thermal expansion coefficient. This was acted as non-radiative recombination center [17]. Therefore, there was a necessity to reduce its dislocations. The solution of GaN with polycrystalline formation of AlN was found by Akasaki et.al (1986) [18, 19].The small thickness of polycrystalline AlN grown on sapphire at low temperature was changed to crystal buffer AlN layer when the raised the temperature at the deposited GaN layer. Buffer AlN layer promoted the nucleation and lateral overgrowth of GaN layer. Nakamura et. al (1992) also reported the low temperature GaN buffer layer [20, 21].

Meanwhile, the formation of PN junction structure is essential to fabricate the LED. GaN that was finished growth step is commonly n-type conductive [22]. N atoms evacuate GaN surface in atmosphere. For this reason, GaN_{1-x} was formed at the surface. However, this n-type conductivity is insufficient to use for commercial electrical devices. Akasaki et.al reported that n-type conductivity of GaN was obtained by using Si atom as dopant [23]. On the other hand, the growth of GaN with p-type conduction was difficult to obtain [24, 25]. Although Pankove selected Zn atom as a p-type dopant of GaN, the insulator characteristic was found. LED was emitted by Metal- Insulator-Semiconductor (MIS) structure. Magnesium (Mg) was also doped in GaN. But, p-type characteristic was not shown [26]. That main reason afterwards discovered was formation of Mg-H complexes [27] Trimethylgallium ($(CH_3)_3Ga$) and ammonia (NH_3) were used as standard precursor, during the growth of GaN. These are contained the Hydrogen (H). H flew into reactor during the growth of Mg-doped GaN was formed the neutral $(Mg\text{-}H)^0$ complexes. Mg captured these

complexes was not activated as acceptor of GaN. As a result, resistivity of Mg-doped GaN show higher than 10^4 Ω·cm [28]. Amano et.al (1989) discovered the p-type conduction of Mg-doped GaN irradiated by the low energy electron beam of electron microscope. This is known as low-energy electron beam (LEEBI) treatment [29]. LEEBI treatment broke the combination of Mg and H. As a result, the activation energy of Mg is decreased. Since then, Nakamura et.al reported that the activation of Mg acceptors can also be achieved by thermal annealing in nitrogen atmosphere [30].

The high conductivity of n- and p-type GaN, the high crystal performance of GaN and growth of InGaN was gradually performed [31].

Eventually, Nakamura et.al (1993) reported a GaN based blue color LED with InGaN/GaN double hetero multi quantum well (MQW) [32, 33]. Realization of a blue color LED was concentrated on research attention of worldwide [34]. Subsequently, the high performance devices were started to develop. For example, laser, indicator, sensor and white LED were reported [35]. LED could be used either for the free-space comun ication applications [36]. Especially, commercialization of white LED with yttrium aluminium garnet (YAG) phosphor was an important application [37]. Demonstration of white LED was created a huge LED illumination market [38].

The research direction is moved to shorter wavelength than blue light. Because, the wavelength range with ultraviolet (UV) ray can widely applicable [39, 40].The sterilization effect of UV light was extensively studied. In medical field, the particular UV wavelength is known the efficient to an atopic dermatitis [41]. UV curing with excimer laser, the lithography equipment with YAG harmonic wave laser was expected to replace the conventional lamp to high performance UV- LED. Besides, UV-LED can apply to the bio-sensor, the photo-catalyst, and white LED [42, 43].

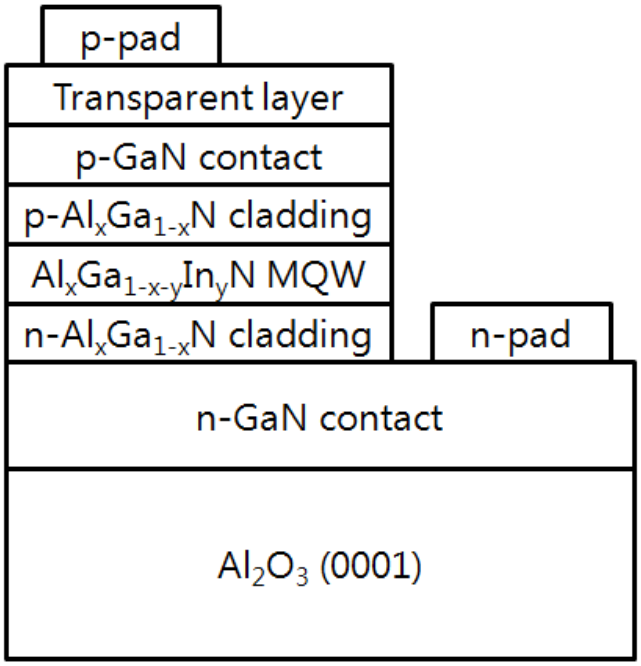

Fig.1 The schematic structure of UV-LED chip.

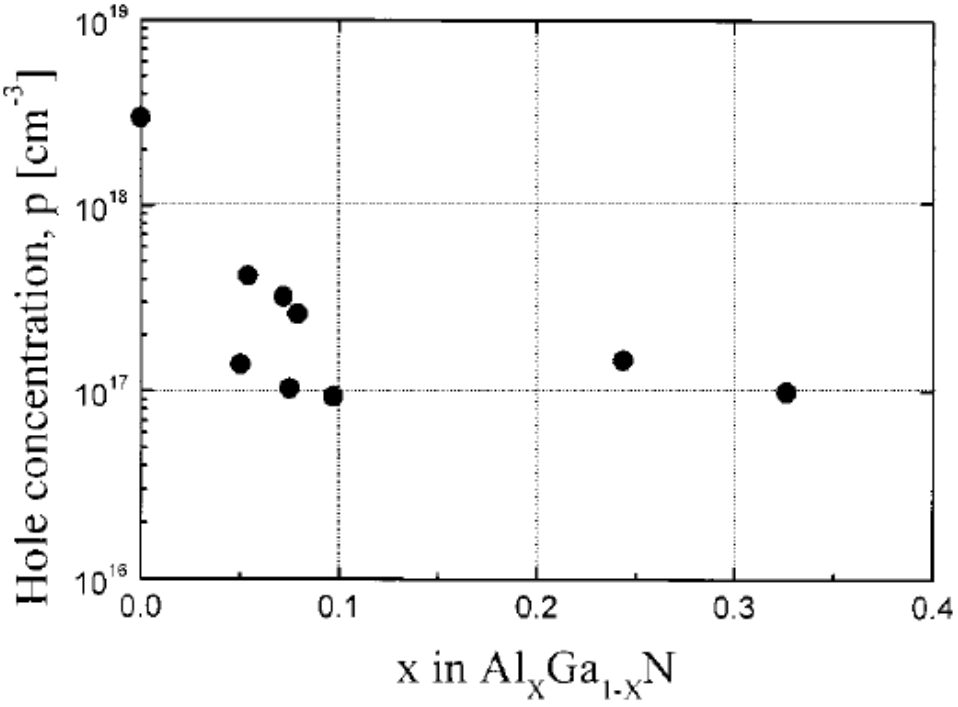

Fig.2 Hole concentration along to Al composition of AlGaN with Mg concentration (10^{19} - 10^{20} cm^{-3}) by Hall measurement [46].

Figure 1 showed typical structure of LED with ultraviolet wavelength. This structure is consist with C-pane sapphire substrate, GaN buffer layer, n-type GaN contact layer, AlGaN:Si electron blocking layer, AlGaInN multi quantum well, AlGaN:Mg hole blocking layer, p-type GaN contact layer and transparent layer. Minimum wavelength of ternary $In_xGa_{1-x}N$ layer is theoretically 365 nm when indium concentration x is 0. In order to obtain the shorter wavelength more than 365 nm, the quaternary $Al_xGa_{1-x-y}In_yN$ layer was selected as an active layer [44, 45].

Figure 2 shows the hole concentration versus AlN mole fraction in AlGaN [46]. The formation of p-type $Al_xGa_{1-x}N$ with high aluminium mole fraction (x) was difficult to obtain. The mobility of Mg-doped AlGaN are decreased with increasing in AlN mole fraction in AlGaN. Even though the injection current was spread by the transparent layer, the current crowding effect was more severe in lateral type ultraviolet LED than the lateral type blue LED. Also, it is reason of increasing in driving current at lateral UV-LED structure. Consequently, the formation of p-type $Al_xGa_{1x}N$ with high aluminium mole fraction (x) should be obtained.

On the other hand, aluminum carbide (Al_4C_3) was known as abrasive material. Al_4C_3 sample grown by MOVPE method have crystallites and absorption band at UV wavelength. Also, carbon (C) was explicitly detected. Al_4C_3 may be solution for formi ng the p-type $Al_xGa_{1-x}N$ with high mole fraction (x) as a new dopant [47]. In this respect, it is necessary to fabricate the UV-LED that is consisted of the p-type $Al_xGa_{1-x}N$ layer doped with Al_4C_3.

1.2 Research purpose

The main objective of this paper is investigation on C-diffusion and the C-doping experiments in AlGaN by Al_4C_3. This is challenge to obtain p-type AlGaN layer with high AlN mole fraction in AlGaN. Also, the photo-induced current and its degradation in Al_4C_3/Al_2O_3 (0001) grown by metalorganic chemical vapor deposition was also researched.

This dissertation is consisted of 5 chapters.

In chapter 1, the recent progress of the III-V nitride and the experimental purposes were briefly introduced.

In chapter 2, the photo-induced current and its degradation in Al_4C_3/Al_2O_3 (0001) are reported. Metalorganic vapor phase epitaxy method was used to grow the Al_4C_3 layer. The growth rate and the consistence of Al_4C_3 were confirmed by scanning electron microscope (SEM) and energy dispersive X-ray (EDX) spectroscopy. The crystallites were analyzed by X-ray diffraction (XRD). The Photo-induced current (PIC) and its degradation in Al_4C_3 layer were investigated by the current-voltage (I-V) and the transmission measurement.

In chapter 3, the high temperature diffusion in AlGaN by Al_4C_3 is performed. The p- and n-type conductivities and carbon intensities in AlGaN with diffusion experiments were measured by Hall, I-V measurement and second ion mass spectrosco py (SIMS) analysis. Also, the relationship of AlC and hole concentration of $Al_{0.45}Ga_{0.55}N$ with diffusion experiment were investigated by X-ray Photoelectron Spectroscopy (XPS).

In chapter 4, C-doped p-AlGaInN LED fabricated from III-V nitride was

grown by metalorganic vapor phase epitaxy by insertion of Al_4C_3/Al_2O_3 (0001). The growth thickness of AlGaN based material was analyzed by SEM. SIMS analysis was used to confirm the concentration of C and Si atoms. I-V and the electroluminescence (EL) measurements were conducted to perform the electrical and the optical characteristics.

Finally, the result of this research is summarized in chapter 5.

Reference

[1] J. Ren, K. A. Bowers, B. sneed, D. L. Dreifus, J. W. Cook Jr., J. F. Schetzina and R. M. Kolbas: Applied Physics Letters **57** (1990) 1901.

[2] D. B. Eason, Z. Yu, W. C. Hughes, W. H. Roland, C. Boney, J. W. Cook Jr., J. F. Schetzina, G. Cantwell and W. C. Harsch: Applied Physics Letters **66** (1995) 115.

[3] M. Hagerott, H. Jeon, A. V. Nurmikko, W. Xie, D. C. Grillo, M. Kobayashi and R. L. Gunshor: Applied Physics Letters **60** (1992) 2825.

[4] H. Jeon, J. Ding, W. Patterson, A. V. Nurmikko, W. Xie, D. C. Grillo, M. Kobayashi and R. L. Gunshor: Applied Physics Letters **59** (1991) 3619.

[5] H. Jeon, J. Ding, A. V. Nurmikko, W. Xie, D. C. Grillo, M. Kobayashi, R. L. Gunshor, G. C. Hua and N. Otsuka: Applied Physics Letters **60** (1992) 2045.

[6] S. Strite and H. Morkoc: J. Vac. Sci.&Technol. **B10** (1992) 1237.

[7] S. Strite, M. E. Lin and H. Morkoc: Thin solid Films **231** (1993) 197.

[8] **増井、Steven、中村**: *LED 2009最新技術と市場動向* (**日経エレクトロニクス**, 東京, 2008), p.6.

[9] **一ノ瀬、田中、島村**: *高輝度LED材料のはなし*, (**日刊工業新聞社**, 東京, 2007), p.12.

[10] M. A. Khan, R. A. Skogman, R. G. Schulze and M. Gershenzon: Appl. Phys. Lett. **43** (1983) 492.

[11] I. Akasaki, H. Amano, Y. Koide, H. Hiramatsu and N. Sawaki: J. Cryst. Growth **98** (1989) 209.

[12] S. Yoshida, S. Misawa and S. Gonda: J. Appl. Phys. **53** (1982) 6844.

[13] S. Nakamura, Y. Harada and S. Seno: Appl. Phys. Lett. **58** (1991) 2021.

[14] J. Karpinski, J. Jum and S. Porowski: J. Cryst. Growth **66** (1984) 1.

[15] S. Nakamura and G. Fasol: *The Blue Laser Diode* (Springer, New York, 1997), p.24.

[16] S. Nakamura and G. Fasol: *The Blue Laser Diode* (Springer, New York, 1997), p.23.

[17] E. F. Shubert: *Light Emitting Diodes* (Cambridge, New York, 2006), p.35.

[18] H. Amano, N. Sawaki and Y. Toyoda: Appl. Phys. Lett. **48** (1986) 353.

[19] H. Amano, I. Akasaki, K. Hiramatsu and N. Koide: Thin Solid Fims **163** (1988) 415.

[20] S. Nakamura, T. Mukai, M. Senoh and N. Iwasa: Jpn. J. Appl. Phys. **31** (1992) L139.

[21] S. Nakamura, N. Iwasa, M. Senoh and T. Muaki: Jpn. J. Appl. Phys. **31** (1992) 1258.

[22] S. Nakamura: Jpn. J. Appl. Phys. **30** (1991) L1705.

[23] N. Koide, H. Kato, M. Sassa, S. Yamasaki, K. Manabe, M. Hashimoto, H. Amano, K. Hiramatsu and I. Akasaki: J. Cryst. Growth **115** (1991) 639-642.

[24] M. Ilegems and R. Dingle: J. Appl. Phys **44** (1973) 4234.

[25] J. I. Pankove and J. A. Hutchby: J. Appl. Phys **47** (1976) 5387.

[26] H. P. Maruska, D. A. Stevenson and J. I. Pankove: Appl. Phys. Lett. **22** (1973) 303.

[27] H. Amano, M. Kito, K. Hiramatsu and I. Akasaki: Jpn. J. Appl. Phys **28** (1989) L2112.

[28] S. Nakamura and G. Fasol: *The Blue Laser Diode* (Springer, New York, 1997), p.111.

[29] S. Nakamura and G. Fasol: *The Blue Laser Diode* (Springer, New York, 1997), p.81.

[30] S. Nakamura, N. Iwasa, M. Senoh and T. Mukai: Jpn. J. Appl. Phys. **31** (1992)

1258.

[31] S. Nakamura and T. Mukai: Jpn. J. Appl. Phys **31** (1992) L1457.

[32] S. Nakamura, T. Mukai and M. Senoh: J. Appl. Phys **76** (1994) L8189.

[33] S. Nakamura, M. Senoh, N. Iwasa, S. Nagahama, T. Yamada and T. Mukai: Jpn. J. Appl. Phys. **34** (1995) L1332.

[34] 酒井: 日経エレクトロニクス,「GaN系青色発光ダイオードの発明について」(1995) p.228.

[35] K. Bando, K. Sakano, Y. Noguchi and Y. Shimizu: Deveolpment of high-bright and pure-white LED lamps, J. Light and Visual Environ, 22. (1998) 2.

[36] E. F. Shubert: *Light Emitting Diodes* (Cambridge, New York, 2006), p.382.

[37] S. Nagahama, N. Iwasa, M. Senoh, T. Matsushita, Y. Sugimato, H. Kiyoku, T. Kozaki, M. Sano, H. Matsumura, H. Umemoto, K. Chocho and T. Mukai: Jpn. J. Appl. Phys. **39** (2000) L647.

[38] 下出: *LED 2009最新技術と市場動向* (日経エレクトロニクス, 東京, 2008), p.50.

[39] 野澤: *LED 2009最新技術と市場動向* (日経エレクトロニクス, 東京, 2008), p.158.

[40] T. Okimoto, M. Tsukihara, K. Kataoka, A. Kato, K. Nishino, Y. Naoi and S. Sakai: Phys. stat. sol. (c) **9** (2008) 3066-3068.

[41] A. Morita, Visual Dermatology **3** (2004) 410.

[42] Y. Muramoto, M. Kimura and S. Nouda: Semicond. Sci. Technol. **29** (2014) 084004

[43] E. F. Shubert: *Light Emitting Diodes* (Cambridge, New York, 2006), p.346.

[44] T. Mukai et. al: Oyo Buturi **68** (1999) 152.

[45] K. Hiramatsu et. al: Oyo Buturi **71** (2002) 204.

[46] M. Katsuragawa, S. Sota, M. Komori, C. Anbe, T. Takeuchi, H. Sakai, H. Amano and I.

Akasaki: J. Cryst. Growth **189/190** (1998) 528.

[47] H. Kawanishi and T. Tomizawa: Phys. Status Solidi B. **249** (2012) 459.

CHAPTER 2

Analysis of Al_4C_3/Al_2O_3 (0001) grown by metalorganic vapor phase epitaxy

2.1 Introduction

In the field of the machinery, Al_4C_3 alloy is particularly well-known material [1]. It is mainly used as an abrasion. This material crystallizes in the rhombohedral or hexagonal systems. In accordance with the value on the Joint Committee on Powder Diffraction Standards (JCPDS) card [2], the lattice constants of the hexagonal system Al_4C_3 were c = 1.5920 nm and a = 0.3408 nm.

Al_4C_3 was typically discovered in the contact of SiC-Al interface by thermal heating [3].Al_4C_3 grow from the solution is separated from each other and constantly subject to a recrystallization process. The reaction could advance until it achieved equilibriu m conditions,since SiC was constantly exposed to aluminium attack. Hexagonal Al_4C_3 was o bserved on Si face of a SiC substrate.

Sintered Al_4C_3 was performed by the hot-pressing method [4]. The micro-Vickers hardness, the four-point bending four point bending, the coefficient of linear thermal expansion and the corrosion resistance to water of Al_4C_3 substantially increased with an increase in the temperature. Thermal expansion of sintered Al_4C_3 was computed to be 43 % at 900 K.

Al_4C_3 formation was formed in the interpenetrating graphite/aluminium composites [5]. Infiltration temperature was critical parameter to the amount of the formed Al_4C_3. The formation of Al_4C_3 grown at 750 ℃ was observed in the eutectic C/$AlSi_{12}$ composite and decreased by reducing the infiltration temperature to 670 ℃. The lath-like interfacial Al_4C_3 crystals in the μm regime was revealed by optical and scanning electron microscopy. The severe degradation of Al_4C_3 was also observed within a few days on composites exposed to ambient conditions.

Al_4C_3 was created by the carbon diffusion in the surface of $AlSi_7Mg_{0.3}$ aluminum alloy (7% silicon and 0.3% magnesium) during the recombination phase of the plasma [6]. Two kinds of ambient gases of methane (CH_4) and propylene (C_3H_6) were chosen to produce the carbon species allowing the carbide layer growth for comparison. By means of the result of X-ray diffraction analysis, the presence of Al_4C_3 was evidenced at the sample surface with no aluminium oxide phase.

Al_4C_3 was also reported for use as a buffer-layer for the self-separation of m-plane GaN by hydride vapor phase epitaxy (HVPE) [7]. Different growth temperature and thickness of Al_4C_3 grown by metalorganic chemical vapor deposition (MOCVD) method was performed to investigate the crystal quality and detachment of the m-plane GaN grown by HVPE method. An Al_4C_3 (0001) layer with a thickness of 20 nm was not degraded, but that with thickness of 70 nm was self- separated. A GaN $(1\bar{1}00)$ layer with a thickness of 500 μm was successfully obtained and that basal stacking fault (BSFs) was $3x10^5$ cm^{-1}.

In addition, Al_4C_3 material was studied in many methods and those achievements were varied [8-13].

Our group has researched and reported on Al_4C_3. Metalorganic vapor phase epitaxy (MOVPE) method was selected to grow this material [14]. The temperature of H_2 annealing was in the range of 1000 to 1150 ℃. The growth temperature of Al_4C_3 layer was in the range of 1000 to 1200 ℃. Trimethylaluminum (TMA) and CH_4 were used as source material. Substrate was Al_2O_3 (0001) with a diameter of 2 inch.

In this paper, we reported the photo-induced current (PIC) in Al_4C_3/Al_2O_3 (0001) [15]. Photo-induced current in Al_4C_3 layer was strongly observed at the ultraviolet light, but these phenomenon deteriorated by the oxidation.

2.2 Experimental procedure

2 inch Al_2O_3 (0001) wafer was chemically cleaned. To improve the growth temperature up to 1200 ℃, the infrared lamp was installed at the sight glass of MOVPE. The light radiation was reached to the suceptor, as shown in Fig.1.

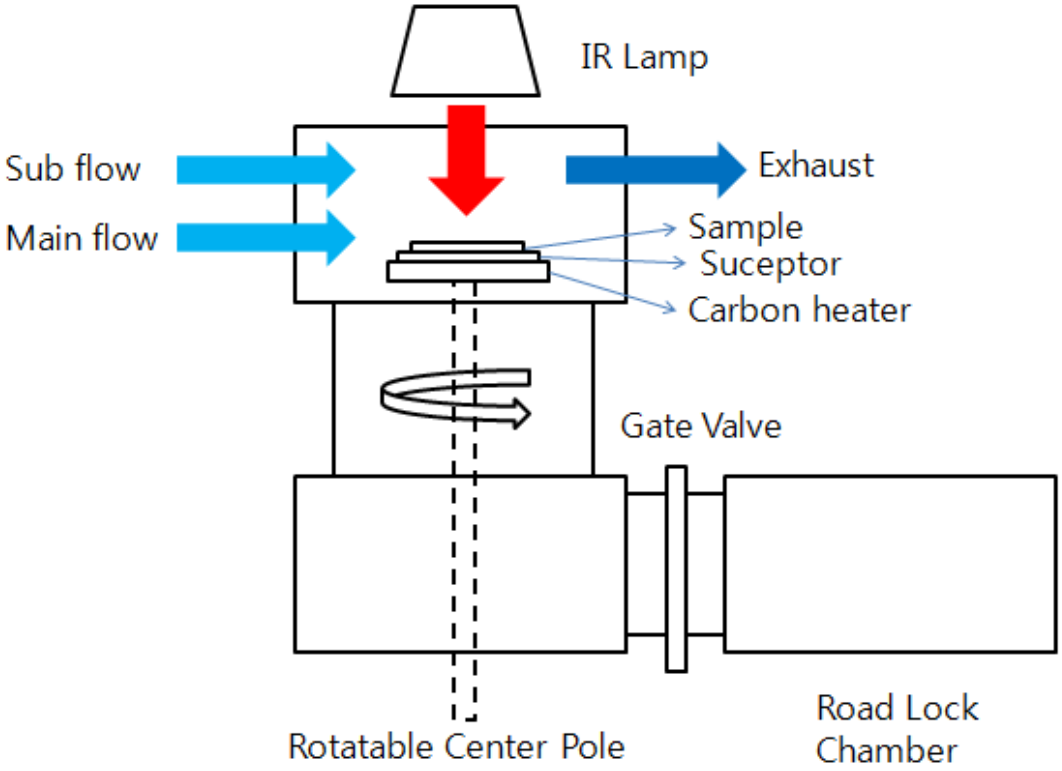

Fig.1 The schematic of MOCVD with IR lamp.

The growth step of Al_4C_3 was conducted, as show in Fig.2. First, the sample was annealed at 1100-1150 ℃ in a H_2 ambient for 10 min. After then, Al_4C_3 growth was performed over a period of 60-120 min. The flow rates of TMA and CH_4 were 33-66 μmol/min and 13.4-26.8 mmol/min. After the growth, Al_4C_3/Al_2O_3 (0001) with a diameter of 2 inch was cut to obtain the pieces of Al_4C_3/Al_2O_3 (0001).

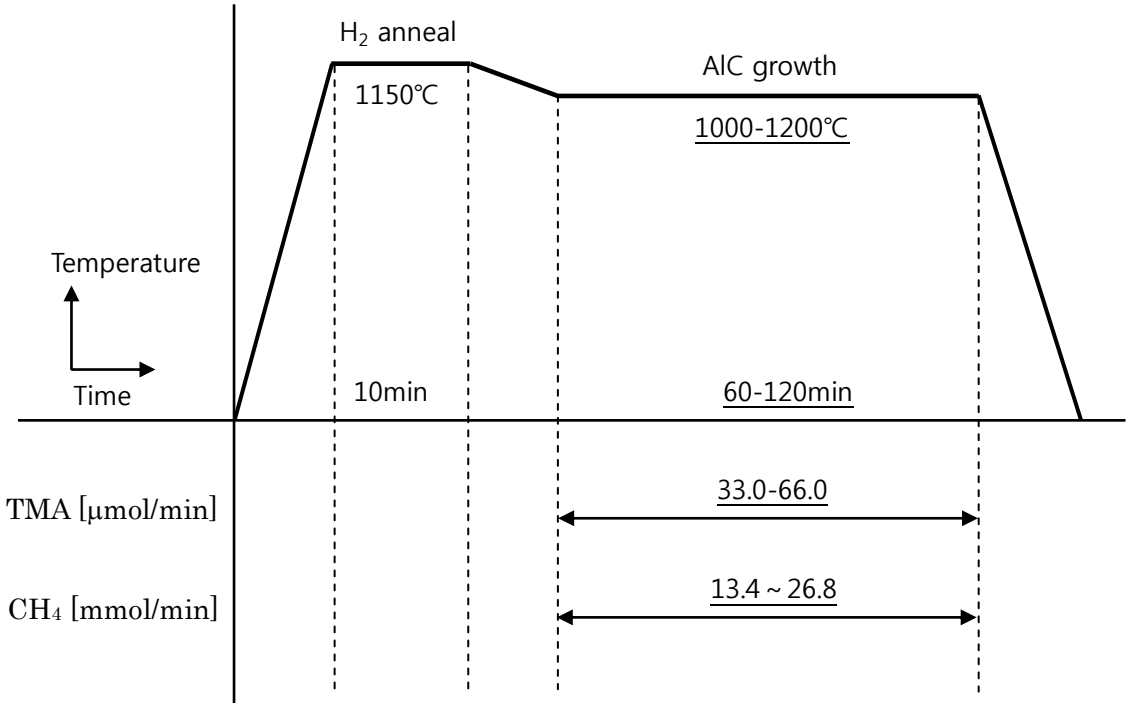

Fig.2 The growth procedure of Al_4C_3.

Growth rate of Al_4C_3 layer was estimated by cross-sectional images of Scanning Electron Microscope (SEM). The acceleration voltage, the probe current and the working distance were 20 kV, 10 nA and 22 mm, respectively. In this condition, the analysis of energy-dispersive X-ray (EDX) spectroscopy was conducted. The image mapping frame rate was 300 frames per second (FPS). X-ray diffraction (XRD) patterns of hexagonal structure Al_4C_3 and Al_2O_3 (0001) were analyzed by 2θ-ω mode.

Grown sample was stored in vacuum condition of 20 Pa. Some pieces were left under air. The evaluation of Al_4C_3 layer was immediately conducted after removal from the vacuum to minimize oxidation.

Xe-lamp which generated photon from around 300 to 900 nm was used in the transmission measurement of Al_2O_3 and Al_4C_3. The wavelength of light transmitted by Al_4C_3 and Al_2O_3 (0001) were analyzed by the spectrometer. With this data, the absorption coefficient of Al_4C_3 was calculated.

To demonstrate PIC experiment, an indium contact was formed on Al_4C_3 layer at 200 ℃. The line width and its spacing were 1 and 5 mm. According to I-V measurement result, the contacts were ohmic.

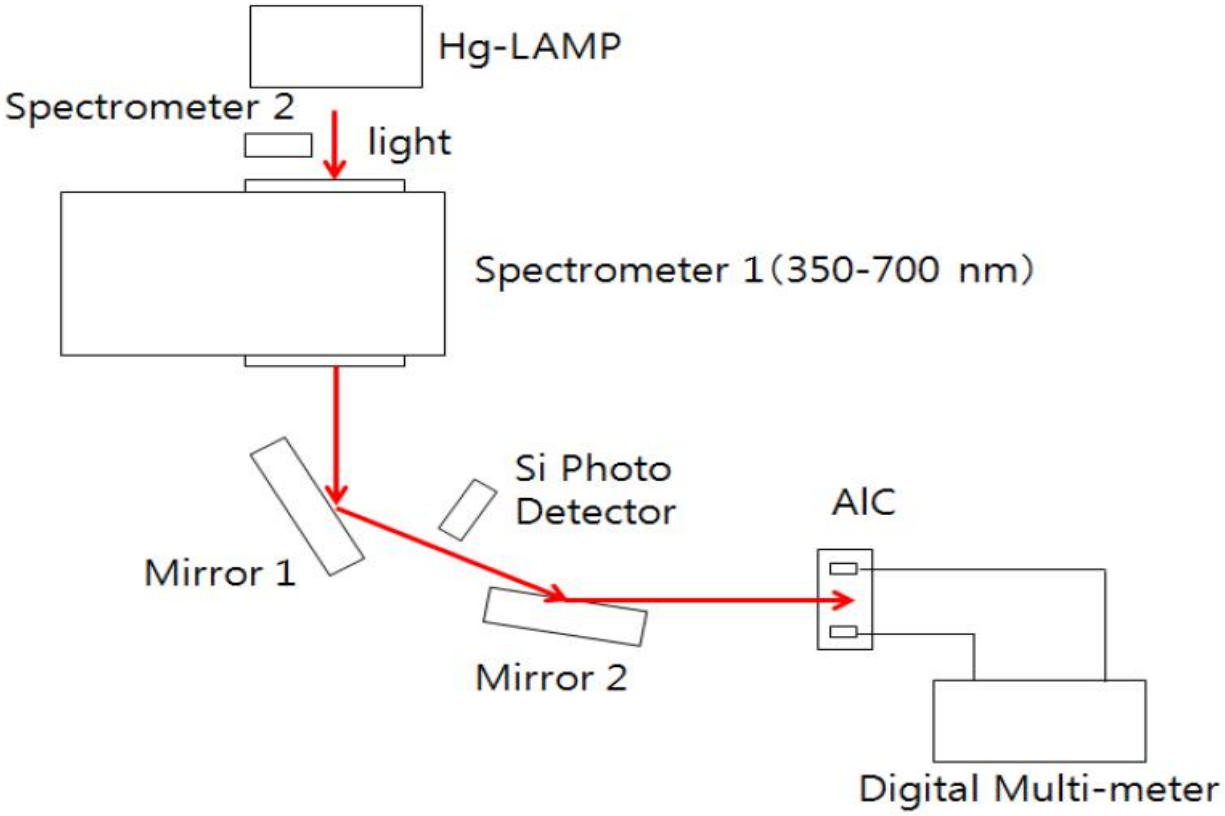

Fig.3 The method of photo-induced current experiment on Al_4C_3/Al_2O_3 (0001).

Hg-lamp, spectrometer 1, spectrometer 2, digital multimeter and Si photo-detector were used to perform the PIC experiment of Al_4C_3/Al_2O_3 (0001), as shown in Fig. 3. Digital

multimeter was used to apply the voltage at each indium electrode. By adjusting spectrometer 2, the strong intensity of Hg-lamp was obtained at 367.6 nm (3.4 eV), 406.7 nm (3.0 eV), 438 nm (2.8 eV), 548.5 nm (2.3 eV) and 580.9 nm (2.1 eV). We selected these wavelengths by spectrometer 1 and the extracted wavelengths were reflected by the mirror. Eventually, the light was projected onto Al_4C_3. The area of the incidental point of light was 1 x 1 cm^2. The current of each wavelength was measured by a Si photo-detector. In this way, we could analyze PIC in Al_4C_3/Al_2O_3 (0001). To detect the deterioration of PIC in the oxidized Al_4C_3/Al_2O_3 (0001), this experiment was repeated after several times.

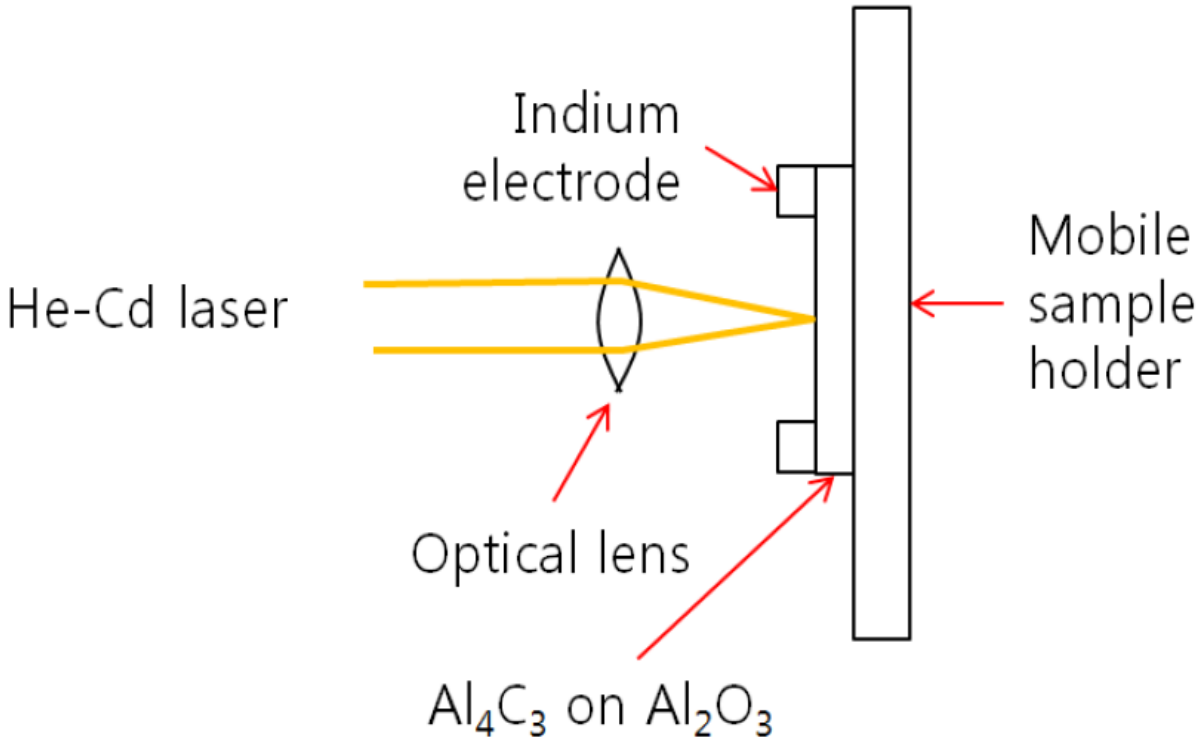

Fig.4 The manner of He-Cd laser-induced current experiment on Al_4C_3/Al_2O_3 (0001).

To confirm whether we were observing a true PIC effect or that of a metal-semiconductor junction, a He-Cd laser with 100 mW of 325 nm peak wavelength was used

as a light source. To focus the laser light at indium contact, the laser light was passed through an optical lens located at a distance of 5 mm from the Al_4C_3 sample, which was fixed on a mobile sample holder and fitted with indium electrodes. We measured the PIC produced by a 50 μm ϕ laser spot across the 0.5 mm spacing between the indium electrodes, as shown in Fig. 4.

2.3 Growth rate and crystallite of Al_4C_3

Figure 5(a) shows the dependence of the growth rate on the growth temperature, TMA and IV/III ratio. The growth rate experiment on the growth temperature was conducted, when the IV/III ratio was 202. A yellowish surface with cleat-shaped Al features was observed at growth temperature below 1000 ℃. The growth rate went up to the 1 μm/h range above 1100 ℃, as shown in Fig. 5(a). The reason was that the CH_4 source gas started to decompose at 1000 ℃ [16]. Figure 5 (b) showed that the growth rate of Al_4C_3 layer was increased with an increase in TMA flow rate, when the flow rate of CH_4 and growth temperature were 26.8 mmol/min and 1150 ℃. At TMA flow rate of 5 to 65 μm/min, the growth rate was calculated in the range of 0.2 to 0.8 μm/h. The growth rate of Fig. 5(c) was significantly decreased with an increase in IV/III ratio. The reason was higher IV/III ratios had a smoother surface morphology.

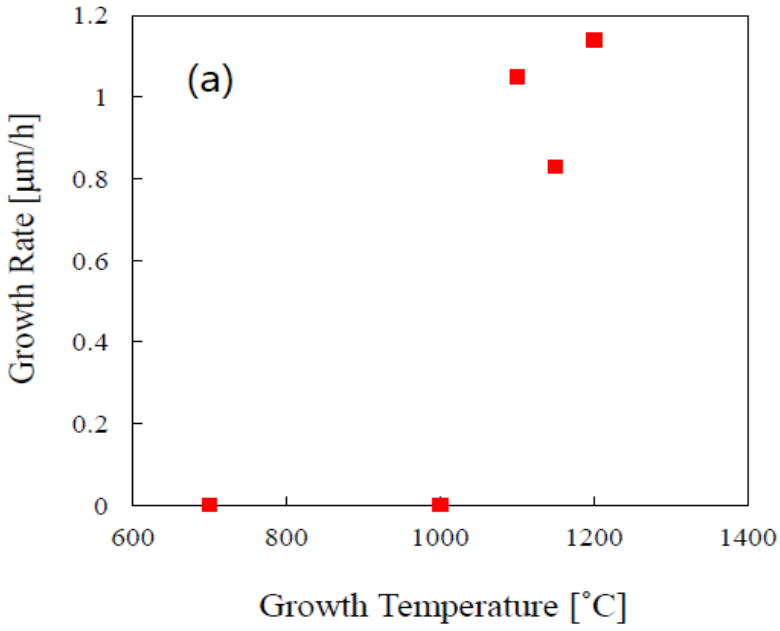

Fig.5(a) Growth rate along c-axis of Al_4C_3 as a function of the growth temperature (IV/III = 202),

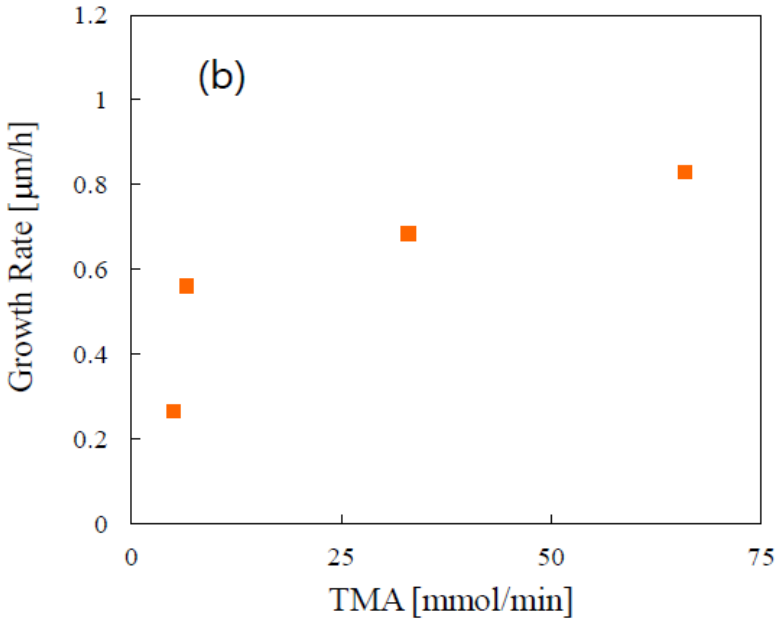

Fig.5(b) Growth rate along c-axis of Al_4C_3 as a function of the amount of TMA (the flow rate of CH_4 = 26.8 mmol/min, the growth temperature = 1150 ℃).

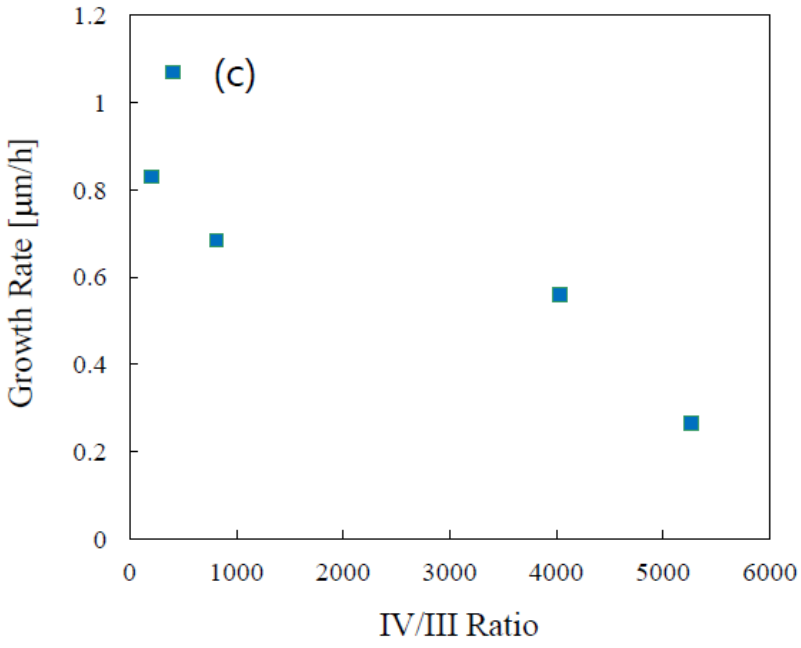

Fig.5(c) Growth rate along c-axis of Al_4C_3 as a function of IV/III ratio (the growth temperature = 1150 ℃)

XRD patterns observed in the 2θ-ω mode for the Al_2O_3 (0001) and hexagonal structure Al_4C_3/Al_2O_3 (0001) grown at 700, 1100 and 1150 ℃ was shown in Fig. 6. Rhombohedral Al_4C_3 peaks were not detected by XRD analysis. The sample grown at 1100 ℃ showed peaks at 32 and 35°. According to JCPDS card, the peaks of 32 and 35° are Al_4C_3 $(2\bar{1}\bar{1}0)$ and Al_4C_3 (0006). Also, the d-spacing of Al_4C_3 $(2\bar{1}\bar{1}0)$ and Al_4C_3 (0006) is 2.952 and 2.650 Å .

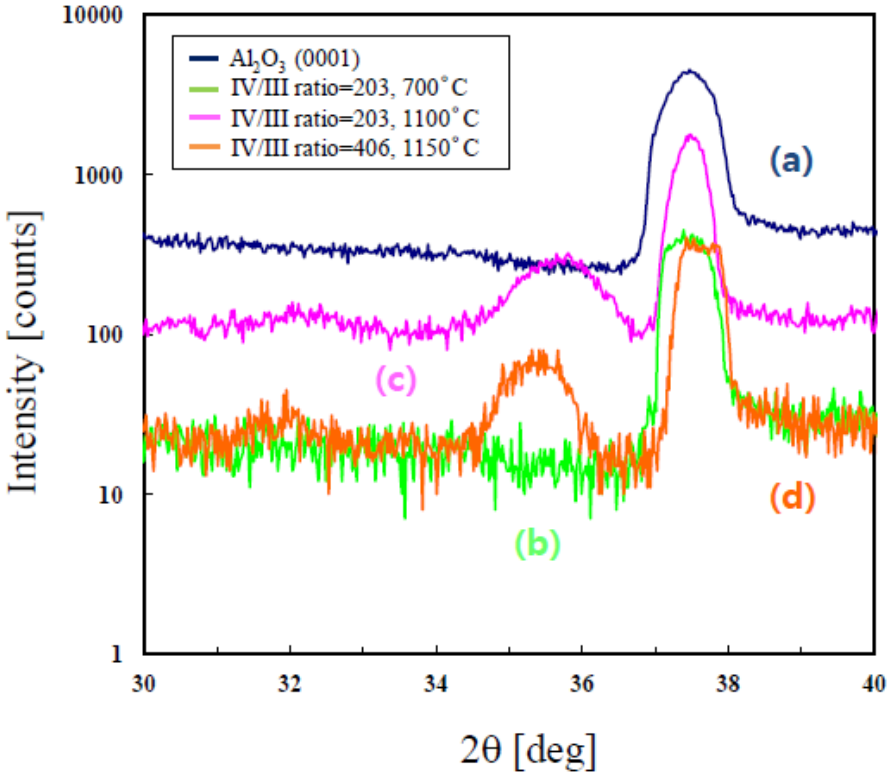

Fig.6 2θ-ω mode of X- ray diffraction that is characteristic of the hexagonal structure of (a) Al_2O_3 (0001) substrate, and Al_4C_3 (0001) layers grown at (b) IV/III ratio = 203, the growth temperature = 700 ℃, (c) IV/III ratio = 203, the growth temperature = 1100 ℃, and (d) IV/III ratio = 406, the growth temperature = 1150 ℃.

2.4 Photo-induced current and its degradation in Al_4C_3/Al_2O_3 (0001)

Al_4C_3 sample was prepared to measure the PIC phenomenon. The growth temperature and the time were 1150 ℃ and 60 min. Also, IV/III ratio was 663. The surface color of the grown sample was yellowish, as shown in Fig. 7(a). But this gradually changed to white with time, as shown in Fig. 7(b). Finally, it separated from substrate at 7 days after the growth. The detachment time of Al_4C_3 was not determined, because of growth condition and oxidation. By storing the sample in vacuum condition, the oxidation of Al_4C_3 sample could be prevented. Despite of the passage of time, the yellow surface color was not changed.

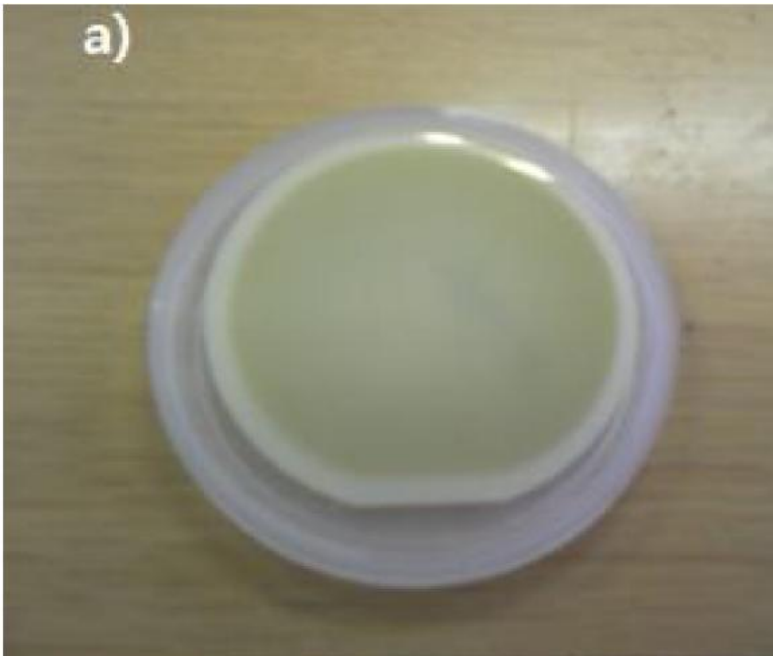

Fig.7(a) Image of a 2 inch Al_4C_3/Al_2O_3 (0001) sample, 1 hour after growth. The growth temperature and time of sample were 1150 ℃ and 60 min. IV/III ratio was 663.

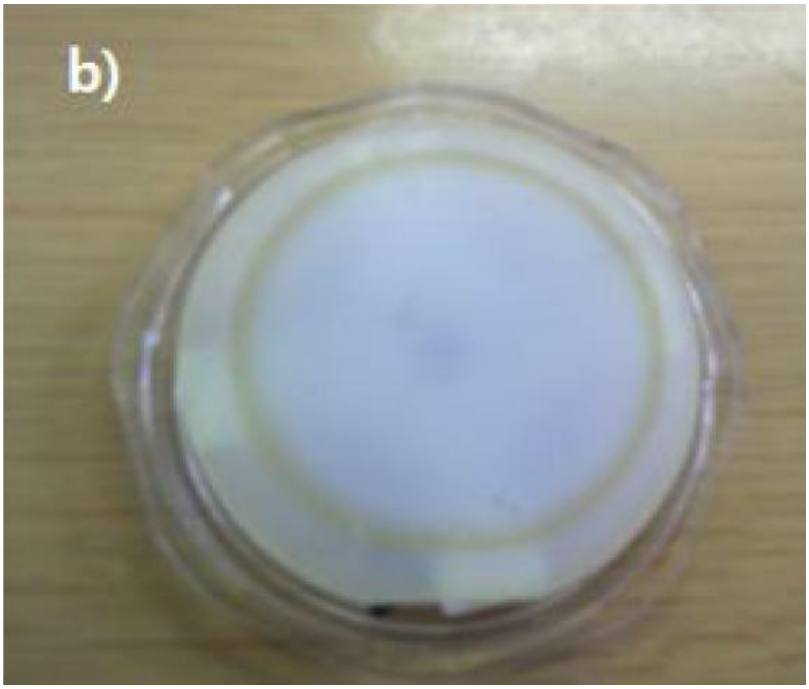

Fig.7(b) Image of a 2 inch Al_4C_3/Al_2O_3 (0001) sample, 7 days after growth. The growth temperature and time of sample were 1150 ℃ and 60 min. IV/III ratio was 663.

These phenomenon again identified by the result of EDX analysis.

Figure 8(a) is a SEM image of an Al_4C_3 layer that was cut in order to scan the cross-sectional direction, and the image was provided by a small angle tilting of the specimen in the Al_4C_3 surface direction. Strong Al and C peaks, and small O peak were shown in Fig. 8(b) and (c), (d). The reason of intensity difference for the same sample was the tilt of analyzed sample. The growth temperature, IV/III ratio, days and thickness of sample 1150 ℃, 812, 3 days and 1 μm. The oxidation of Al_4C_3 was obtained in samples for at least 3 days after the growth.

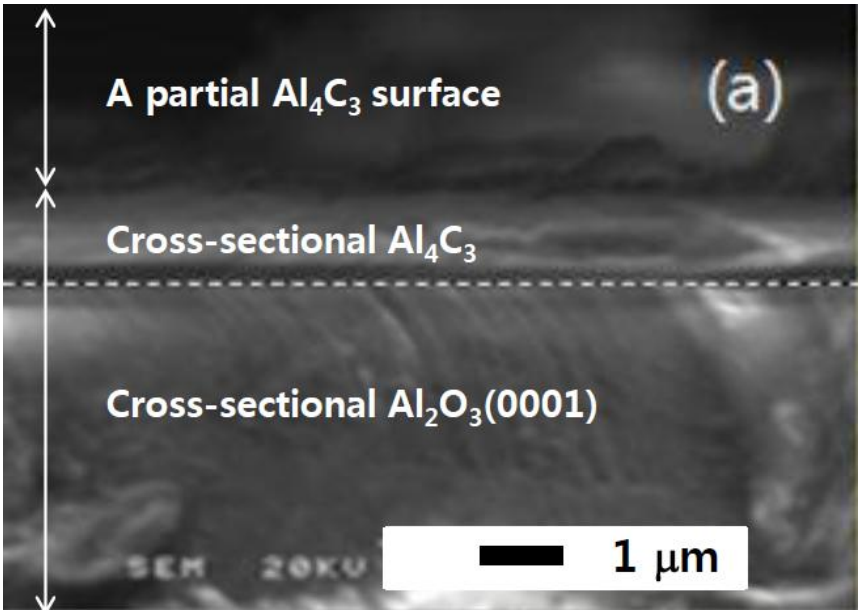

Fig.8(a) SEM image of Al_4C_3/Al_2O_3 (0001). Elapsed time of sample is 3 days after growth. The growth temperature, IV/III ratio, and thickness were 1150 ℃, 812, and 1 μm, respectively.

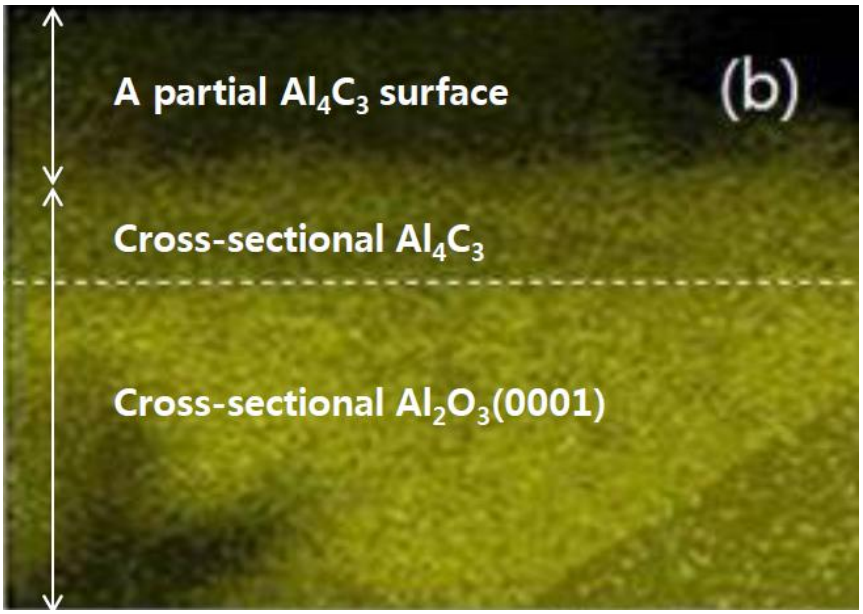

Fig.8(b) EDX characteristics of Al. Elapsed time of sample is 3 days after growth. The growth temperature, IV/III ratio, and thickness were 1150 ℃, 812, and 1 μm, respectively.

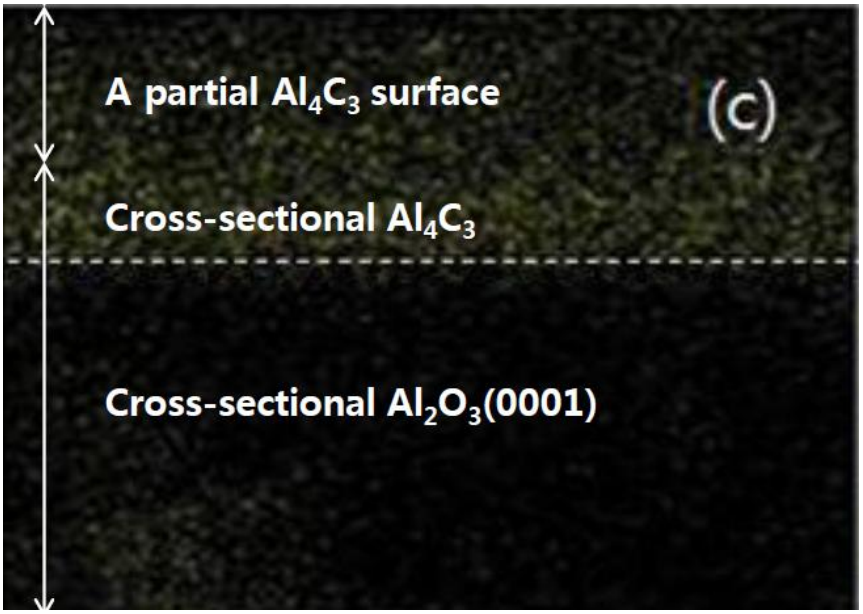

Fig.8(c) EDX characteristics of C. Elapsed time of sample is 3 days after growth. The growth temperature, IV/III ratio, and thickness were 1150 ℃, 812, and 1 μm, respectively.

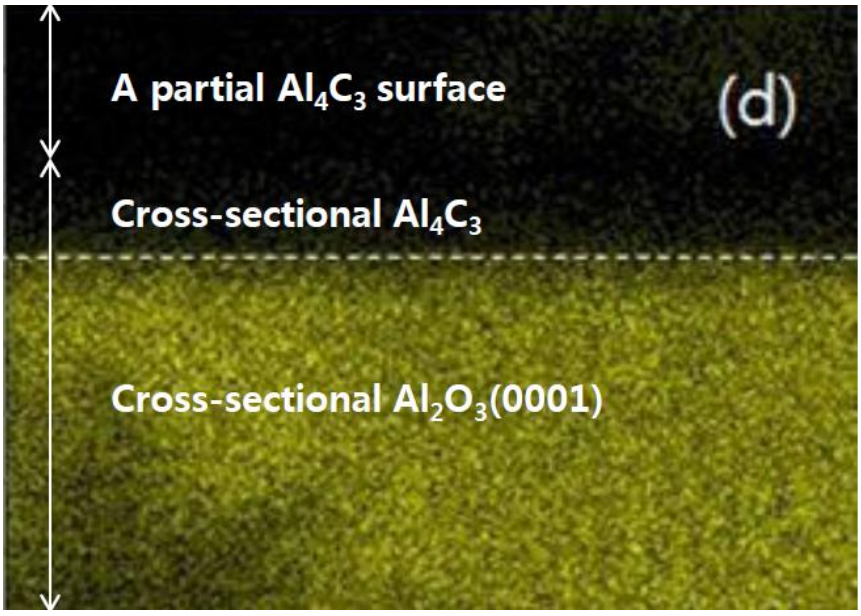

Fig.8(d) EDX characteristics of O. Elapsed time of sample is 3 days after growth. The growth temperature, IV/III ratio, and thickness were 1150 ℃, 812, and 1 μm, respectively.

The transmission experiment was conducted to calculate the absorption coefficient of Al_4C_3 as shown in Fig. 9. The experimental absorption coefficient was computed from the following formula,

$$\alpha = A(h\nu / E_g)^{1/2} \quad (cm^{-1}) \quad (1)$$

where α is the absorption coefficient, h is Plank's constant, ν is the frequency and E_g is the bandgap energy, respectively. The absorption coefficient reached to 10^4 cm^{-1} at the peak of the absorption band, but it gradually decreased towards visible wavelengths. This gradual decrease agreed with the yellowish color sample to the human eye.

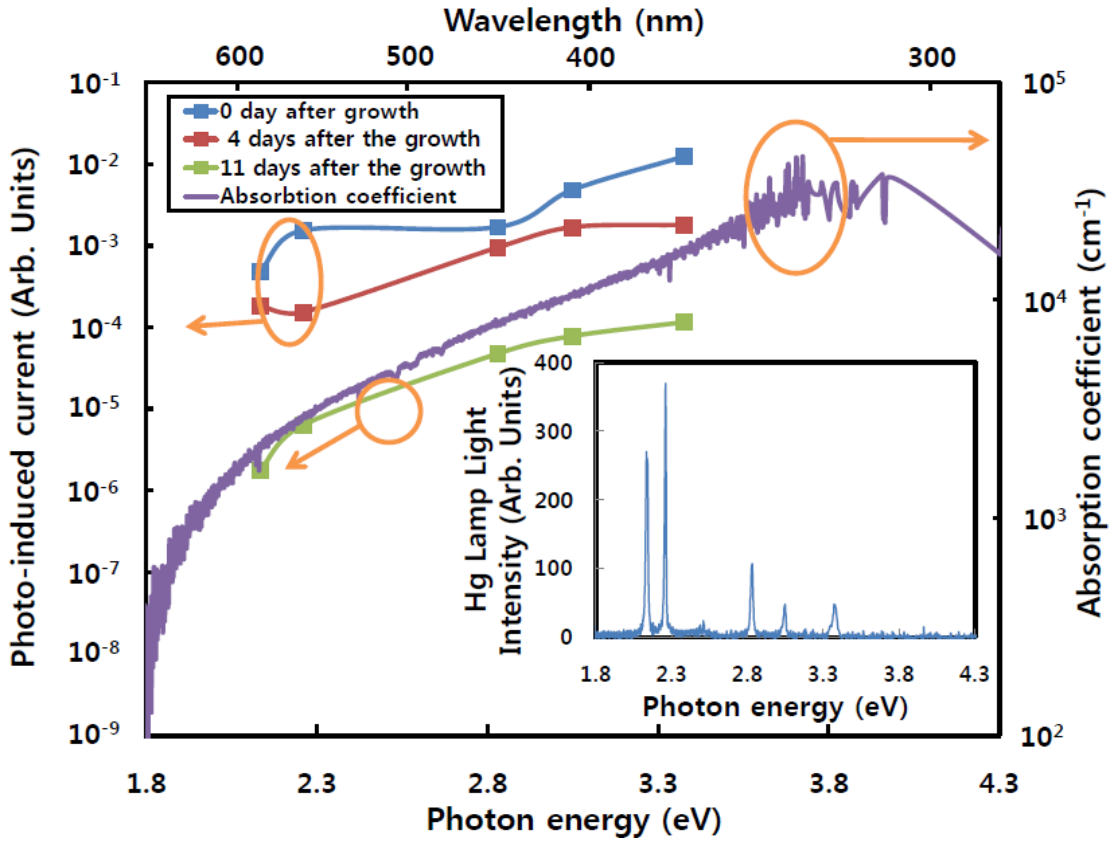

Fig.9 Photo-induced current and experimental absorption coefficient of Al_4C_3/Al_2O_3 (0001). The inset is the Hg-lamp light peak as a function of photon energy.

The PIC experiment was conducted to confirm the bandgap of Al_4C_3. Selected wavelength that had higher photon energy than 1.8 eV except the effect of the deep level transition. The obtained PIC was shown in Fig. 10. The dark current and PIC with 367.6 nm at 30 V were at 29 and 14 nA, respectively. Dark current was clearly increased by the light irradiation.

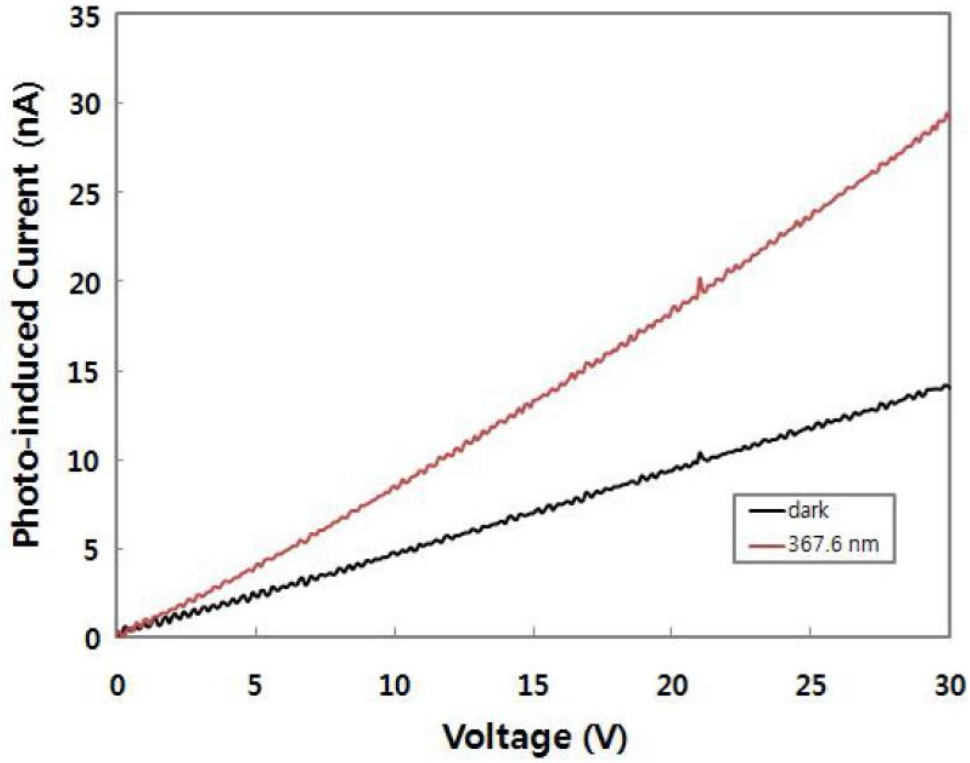

Fig.10 Change in PIC with 367.6 nm irradiation and dark current in Al_4C_3/Al_2O_3 (0001) with respect to the applied voltage. The growth temperature and the time of sample were 1150 ℃ and 60 min. IV/III ratio was 663.

We also checked the effect of other wavelengths. The wavelengths of 367.6, 406.7, 438, 548.5 and 580.9 nm were used to confirm PIC in Al_4C_3/Al_2O_3 (0001). These wavelengths were strong intensities in Hg-lamp, as shown in Fig. 9. To compare the PIC, we prepare the 0, 4 and 11 days sample after the growth

experiment. The following was the formula of photo-conduction that occurred with incident photons.

$$\text{photo} - \text{conduction} = \frac{\text{PIC at 30 [V]} - \text{dark current at 30 [V]}}{\text{Current of the wavelength measured by a Si PD} \times \text{Si PD sensitivity at each wavelength}} \quad (2)$$

The photo-conduction and absorption coefficient in Al_4C_3/Al_2O_3 (0001) was shown in Fig. 9. Figure 11 shows the sensitivity of Si photo diode. The experimental absorption coefficient of Al_4C_3 was calculated by the transmission result of Al_4C_3/Al_2O_3 (0001). Sample for transmission experiment was used that was immediately finished growth procedure in MOVPE. Regardless of elapsed time, the photo-conduction increased with a decreased in the extracted wavelength. This indicated PIC is sensitive to shorter wavelength.

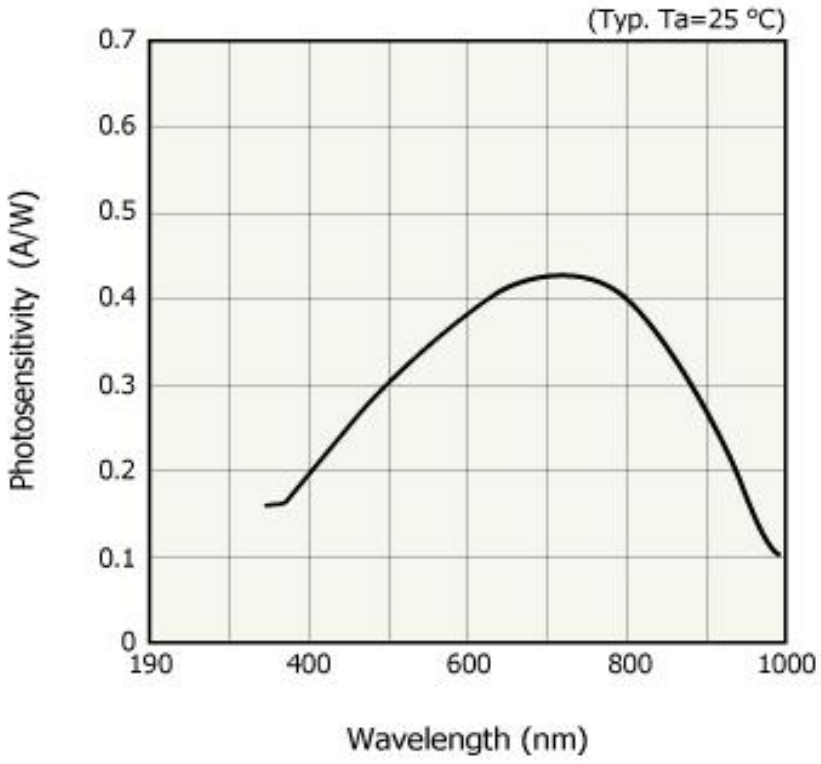

Fig.11 The sensitivity of Si photo diode.

Figure 9 shows the absorption coefficient and photo- conduction in Al_4C_3/Al_2O_3 (0001) by oxidation. In the case of 2.1 eV photons, the measured PIC for material 0, 4 and 11 days after growth were 4 x 10^{-4}, 1 x 10^{-4} and 1 x 10^{-6} (Arb. Units), respectively. In case of PIC at 3.4 eV photons, the measured PIC for material 0, 4 and 11 days after growth were 1 x 10^{-2}, 1 x 10^{-3} and 1 x 10^{-4} (Arb. Units), respectively. Besides, the PIC and dark current are also different. The 11 day-old sample is in the range of 10 nA, but the 0 and 4 days after grow t h samples is in the range of 10^{-8} A. The degradation r e a s o n of photo-conduction was oxidation. This can be easily inferred from Fig. 7(a) and (b).

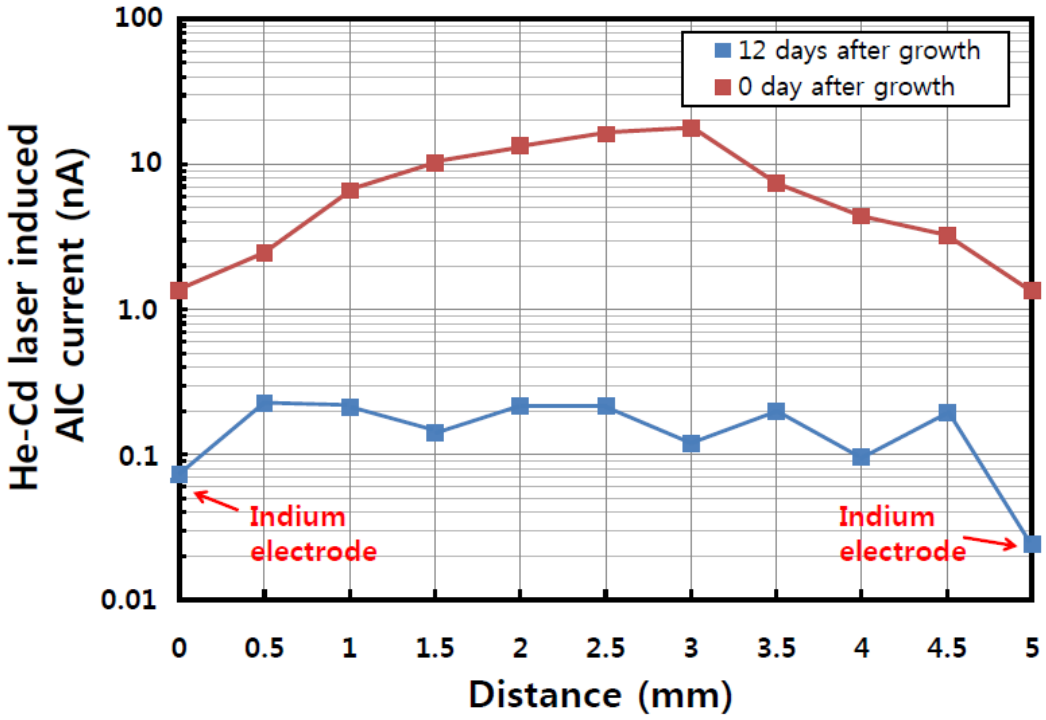

Fig.12 Change of He-Cd laser-induced current along the material separating indium contact.

The PIC result of Al_4C_3/Al_2O_3 (0001) across the material separating between two indium electrodes (5 mm) was shown in Fig. 12. The contact points of the electrode had a small PIC compared with other points. The small signal decrease near the electrodes

is from masking the laser beam by the electrodes. This is very critical in this point. Also, this was observed on the 0 days as well as the 12 days after growth. If the conduction was a metal-semiconductor junction phenomenon, the points that were contacting electrodes should have a large PIC value compared to the other points. But, the experimental result was exactly different. In this reason, metal-semiconductor contact not main reason for this phenomenon. The maximum PIC value of 0 days after growth sample was 17.6 nA. PIC was not constant, because of non-uniform resistance in Al_4C_3 layer. The fluctuation of PIC was confirmed for the 12 day old sample. PIC decreased with increase in time. The PIC difference between the 0 and 12 days after growth samples was more than 10 times over the entire area.

2.5 Summary

In this research, we reported the photo-induced current and its deterioration by oxidation in Al_4C_3/Al_2O_3 (0001). The photo-induced current of Al_4C_3 was not related to the existence of a metal-semiconductor junction. This phenomenon sharply increased with a decrease in wavelength. However, this characteristic was diminished with the oxidation of Al_4C_3. The degradation of sample was confirmed in atmosphere. The surface of Al_4C_3 neglected in air slowly changed to white and it finally separated from the Al_2O_3 (0001). On the other hand, the surface of Al_4C_3 stored in vacuum condition kept yellow color. It was same color of sample that was immediately finished growth. The PIC characteristic of Al_4C_3 can be applied for use as a light sensor in equipment kept in vacuum or other gases which do not contain oxygen.

Reference

[1] Y. Ozcatalbas: Compos. Sci. Technol. **63** (2003) 53.

[2] Card No. 50-0740, ICDD, PCPDFWIN v.2.1. JCPDS, JCPDS-International Centre for Diffraction Data, 2000.

[3] J. C. Viala, F. Bosselet, V. Laurent and Y. Lepetitcorps: J. Mater. Sci. **28** (1993) 5301.

[4] T. Iseki, T. Kameda, T. Maruyama, J. Mater. Sci. Lett. 2 (1983) 675.

[5] T. Etter, P. Schulz, M. Weber, J. Metz, M. Wimmler, J. F. Löffler, P. J. Uggowitzer, Mater. Sci. Engin A. **448** (2007) 1.

[6] F. Fariaut, C. Boulmer-Leborgne, E. Le Menn, T. Sauvage, C. Andreazza-Vignolle, P. Andreazza and C. Langlade: Appl. Surf. Sci. **186** (2002) 105.

[7] H. Sasaki, H. Sunakawa, N. Sumi, K. Yamamoto, A. Usui, Phys. Status Solidi A. **206** (2009) 1160.

[8] C. Qiu and R. Metselaar: J. Am. Ceram. Soc. **80** (1997) 2013.

[9] L. Hong, R. M. Vilar and W. Youming: J. Mater. Sci. **32** (1997) 5545.

[10] J. A. Vreeling, V. Ocelík, G. A. Hamsta, Y. T. Pei, J. Th and M. De Hosson: Scr. Mater. **42** (2000) 589.

[11] G. Carotenuto, A. Gallo and L. Nicolais: J. Mater. Sci. **29** (1994) 4967.

[12] J. Leis, A. Perkson, M. Arulepp, M. Käärik and G. Svensson: Carbon **39** (2001) 2043.

[13] A. Ureña, J. M. Gómez De Salazar, L. Gil, M. D. Escalera and J. L. Baldonedo: J. Microsc. **196** (1999) 124.

[14] D. Kim, F. Horie, Y. Onishi, Y. Naoi and S. Sakai, International Conference Metal

Organic Vapor Phase Epitaxy (2012) TuP-71.

[15] D. Kim, Y. Onishi, R. Oki and S. Sakai: Thin Solid Films **557** (2014) 216.

[16] M. Frenklach: J. Appl. Phys. **65** (1989) 5142.

[17] Hamamatsu Photonics Si photo diode (Model KSPDB00307EA).

CHAPTER 3

High temperature diffusion in AlGaN by Al_4C_3

3.1 Introduction

Near-ultraviolet wavelength less than 350 nm has been researched for a long time [1]. But, the maximum external quantum efficiency (EQE) of Al_xGa_yN based- LED with near-UV (300-340 nm) is less than 8%. Deep-UV (less than 280 nm) is less than 16% [2]. That main reason is that p-type activation in $Al_xGa_{1-x}N$ is low [3]. In the case of n-type AlGaN with a Si dopant, it is possible to keep the concentration of free electrons up to the fraction of AlN. But, in the case of p-type AlGaN with a Magnesium (Mg) dopant, it is hard to exceed Al ($x \geqq 0.33$) mole fraction in AlGaN [4].

To resolve this problem, the research of carbon-doped GaN was challenged [5-7]. The electrical and optical behaviors of C doping were studied by co doping carbon with silicon [8]. By secondary ion mass spectrometry (SIMS) analysis, the abrupt doping profile of C incorporation was observed to be as high as 1×10^{19} cm^{-3}. Also, the growth rate, mode, and structure of GaN that was grown by rf-plasma molecular beam epitaxy (MBE) were not affected by tetrabromomethane (CBr_4).

By using acetylene (C_2H_2) as the dopant, C-doped $(1\bar{1}01)$ AlGaN was obtained [9]. Two near-band-edge emission peaks of the donor bound exciton and a carbon-related exciton peak were detected in cathode luminescence (CL) spectra at 4.2 K. Optical properties of $(1\bar{1}01)$ AlGaN:Mg have been analyzed to compare $(1\bar{1}01)$ AlGaN:Mg with $(1\bar{1}01)$ AlGaN:C.

But, p-type conductivity was not achieved. Recently, a LED structure with C-doped $Al_{0.27}Ga_{0.73}N$/u-GaN/Si-doped $Al_{0.10}Ga_{0.90}N$ was reported [10]. P-type conductivity in C-doped (0001) plane AlGaN layer was obtained by Al mole fraction of 55 %. The maximum net ionized acceptor densities (NIAD) for $Al_xGa_{1-x}N$ were all in the range of (6-7) $\times$ 10^{18} cm^{-3}.

Al_4C_3 grown by metalorganic vapor phase epitaxy (MOVPE) method was reported in chapter 2 [11]. By energy dispersive X-ray (EDX) spectroscopy, C peak was strongly detected in the cross-section Al_4C_3/Al_2O_3 (0001). In this chapter, Al_4C_3 sample was used as carbon diffusion material and was diffused in AlGaN sample to obtain the AlGaN with the p-type conductivity [12].

3.2 Experimental procedure

2 inch Al_4C_3/Al_2O_3 (0001) of 1 µm was cut to a size of 1 x 1 cm^2 by the diamond pencil. $Al_xGa_{1-x}N$ (x = 0.00, 0.04, 1.00) samples were also prepared in the usual way: GaN/ buffer-GaN layer (22 nm)/Al_2O_3 (0001), $Al_{0.04}Ga_{0.96}N$/buffer- GaN layer (19 nm)/ Al_2O_3 (0001) and AlN/buffer-AlN layer (15 nm)/Al_2O_3 (0001), respectively. $Al_xGa_{1-x}N$ (x = 0.45, 0.65, 0.85) samples were grown by modified migration enhanced epitaxy (MEE) method [13] : $Al_{0.45}Ga_{0.55}N$/MEE-buffer- AlN layer (22 nm)/Al_2O_3 (0001), $Al_{0.65}Ga_{0.35}N$/ MEE-buffer-GaN layer (19 nm)/Al_2O_3 (0001) and $Al_{0.86}Ga_{0.14}N$/MEE-buffer- AlN layer (15 nm)/ Al_2O_3 (0001), respectively. The growth times of GaN, $Al_{0.04}Ga_{0.96}N$, $Al_{0.45}Ga_{0.35}N$, $Al_{0.65}Ga_{0.35}N$,$Al_{0.86}Ga_{0.14}N$ and AlN layer were 50, 60, 30, 30, 30 and 60 min, respectively. Also, the growth temperatures of GaN, $Al_{0.04}Ga_{0.96}N$, $Al_{0.45}Ga_{0.35}N$, $Al_{0.65}Ga_{0.35}N$, $Al_{0.86}Ga_{0.14}N$ and AlN sample were at 1075, 1075, 1100, 1160, 1160 and 1160 ℃, respectively.

In this diffusion experiments, the low pressure-MOVPE system was used. Al_4C_3 layers were positioned, face by face, on each $Al_xGa_{1-x}N$ sample that was located on the suceptor. Two diffusion conditions; 1000 ℃, 40 min and 100 Torr (called 1000 ℃) and 1100 ℃, 60 min, 500 Torr (called 1100 ℃); were performed on $Al_xGa_{1-x}N$ (x = 0.00, 0.04,

0.45, 0.65, 0.86, 1.00) samples to compare a calculated diffusion coefficients of C, respectively. The flow rate of NH_3 was 143 mmol/min. Also, the suceptor was rotated in this experiment. The temperature was then downed to room temperature, and the characteristics of each $Al_xGa_{1-x}N$ sample were evaluated.

To perform van der Paw method, $Al_xGa_{1-x}N$ samples were cut to the size of 1 x 1 cm^2 by the diamond pencil. Ti (30 nm)/Al(300 nm) was evaporated on $Al_xGa_{1-x}N$ samples without diffusion experiment. Annealing was performed in N_2 atmosphere at 410 ℃ for 20 min. On the other hand, Ni (10 nm)/Au(10 nm) was evaporated on $Al_xGa_{1-x}N$ samples after the diffusion experiments and then annealed in N_2 atmosphere at 520 ℃ for 10 min. Hall measurement was performed. Measurement temperature, magnetic intensity, and the current were 300 [K], 0.1 [T], and 1 mA, respectively.

Second ion mass spectroscopy (SIMS) analysis was used to confirm the C-concentration into $Al_xGa_{1-x}N$ (x = 0.00, 0.04, 0.45, 0.65, 1.00) samples. The carbon concentration was estimated by 6H-SiC (0001)substrate which is already known the number of carbon composition per cm^{-3}.

X-ray photoelectron spectroscopy (XPS) measurement was selected to confirm the C-diffusion mechanism. $Al_xGa_{1-x}N$ (x = 0.00, 045, 0.65) sample with diffusion condition at 1000 ℃ and $Al_{0.45}Ga_{0.55}N$ sample with diffusion condition at 1100 ℃ was analyzed.

3.3 Hall measurement

The results of Hall measurement were shown in Table I. The un-annealed samples of $Al_xGa_{1-x}N$ ($x \leqq 0.45$) were n-type conductivity, but this characteristic was distinctly changed to p-type conductivity for $x \leqq 0.45$ after the diffusion condition at 1000 ℃, except

GaN sample. This result was also founded in $Al_{0.45}Ga_{0.55}N$ sample with diffusion condition at 1000 ℃.

Table I The result of Hall effect measurement at 300 [K]. The thickness of p-type AlGaN layer formed by diffusion experiment was assumed to be 200 nm.

Al composition (x) of $Al_xGa_{1-x}N$ samples	Before Diffusion			After Al_4C_3 Diffusion					
				1000℃, 100 Torr, 40 min			1100℃, 500 Torr, 60 min		
	n, p (cm^{-3})	μ_H ($cm^2/V{\cdot}S$)	ρ (Ω·cm)	*n, p* (cm^{-3})	μ_H ($cm^2/V{\cdot}S$)	ρ (Ω·cm)	*n, p* (cm^{-3})	μ_H ($cm^2/V{\cdot}S$)	ρ (Ω·cm)
0.00	$n = 2 \times 10^{17}$	362	0.11	$n = 1 \times 10^{17}$	242	0.20	-	-	-
0.04	$n = 3 \times 10^{17}$	105	0.19	$P \geqq 3 \times 10^{18}$	102	0.02	x	x	x
0.45	$n = 1 \times 10^{17}$	91	0.05	$P \geqq 1 \times 10^{18*}$	150*	0.04*	$p \geqq 3 \times 10^{18*}$	3*	0.04*
0.65	-	-	-	-	-	-	-	-	-
0.86	-	-	-	-	-	-	-	-	-
1.00	-	-	-	-	-	-	-	-	-

- : Not enough current value

x : Not measured

*It is not exact.

The hole concentration (*p*) was dependent on the thickness of the sample. At depth 200 nm, the hole concentration of $Al_{0.04}Ga_{0.96}N$ and $Al_{0.45}Ga_{0.55}N$ samples with diffusion condition at 1000 ℃ was evaluated 3 x 10^{18} and 1 x 10^{18} cm^{-3}, respectively. Also, the hole concentration of $Al_{0.45}Ga_{0.55}N$ sample with diffusion condition at 1100 ℃ was calculated 3 x 10^{18} cm^{-3}. But, the mobility of AlGaN samples was complex. The mobility of p-$Al_{0.45}Ga_{0.55}N$

sample with diffusion condition at 1000 ℃ was 150 cm^2/V.s, but that of n-$Al_{0.45}Ga_{0.55}N$ sample without diffusion experiment was 91 cm^2/V.s. We assumed that the main reason is n-AlGaN layer located under the p-type AlGaN layer formed by the diffusion of Al_4C_3 layer [14]. As a result, the150 cm^2/V.s is obtained.

In fact, van der Paw method is useful to determine p- or n- type concentration, but it is meaningless to calculate the concentration or the hole the concentration or the mobility are meaningful. The resistivity of AlGaN samples confirmed as p- type conductivity was estimated in the range of 0.02 ~ 0.04 Ω.cm at 300 [K]. That is smaller value than the low energy electron-beam irradiation treated Mg-doped GaN layer [15].

$Al_xGa_{1-x}N$ ($x \geqq 0.65$) samples needs to find the ohmic contact condition. For example, the current value of $Al_{0.65}Ga_{0.35}N$ sample with the diffusion condition at 1000 ℃ was confirmed at 10^{-6} [A] for 10 [V] by I-V measurement. It is not enough current value to measure the voltage value in Hall measurement.

GaN and AlN samples with diffusion experiment were n- type and insulator, while the $Al_xGa_{1-x}N$ ($x \leqq 0.45$) samples with diffusion condition at 1000 ℃ were clearly p-type conductivities. The GaN C-diffused at 1100 ℃ was an insulator.

3.4 SIMS analysis

The C-concentration in $Al_xGa_{1-x}N$ diffused by Al_4C_3 layer was profiled by SIMS analysis. Profiling depth of GaN, $Al_{0.04}Ga_{0.96}N$, $Al_{0.45}Ga_{0.55}N$ and $Al_{0.65}Ga_{0.35}N$ samples with diffusion condition at 1000 ℃ were confirmed as 1.8, 0.8, 0.8 and 0.8 μm, respectively. Also, etched depth of AlN sample with diffusion condition at 1100 ℃ was 0.22 μm.

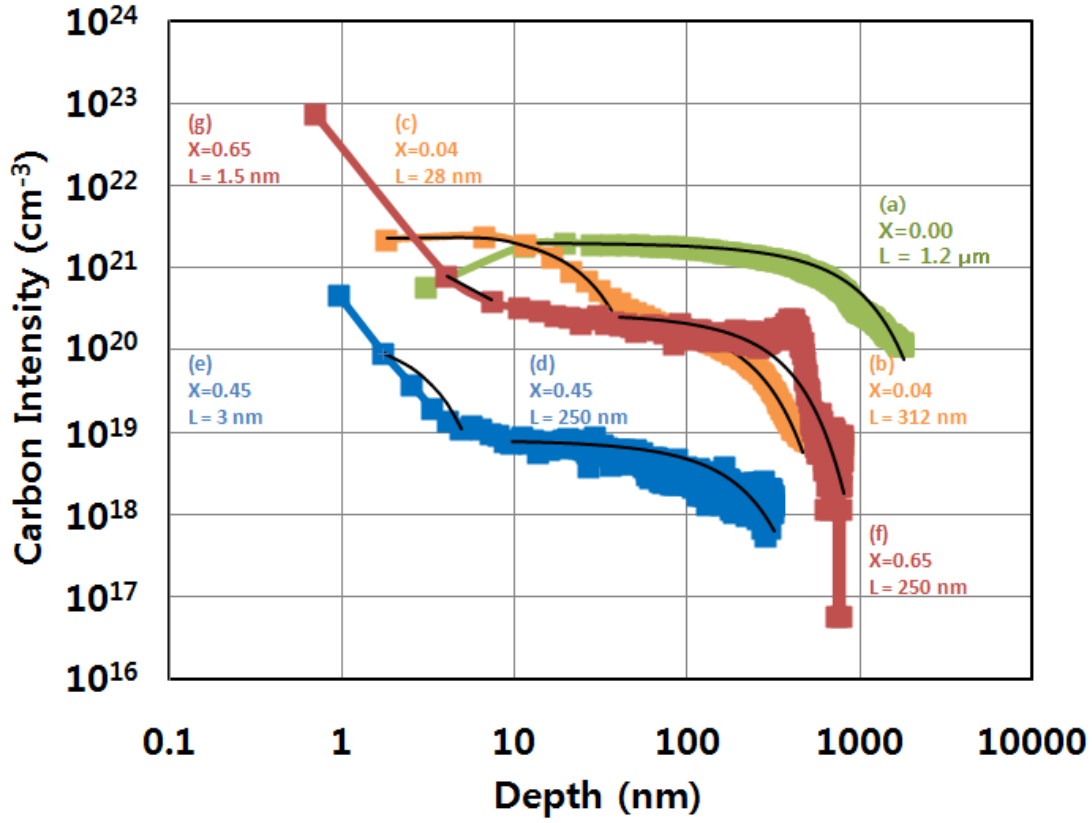
Carbon Intensity (cm-3)
10^24
10^23
10^22
10^21
10^20
10^19
10^18
10^17
10^16
0.1
1
10
100
1000
10000
Depth (nm)
(g)
X=0.65
L = 1.5 nm
(c)
X=0.04
L = 28 nm
(a)
X=0.00
L = 1.2 µm
(e)
X=0.45
L = 3 nm
(d)
X=0.45
L = 250 nm
(b)
X=0.04
L = 312 nm
(f)
X=0.65
L = 250 nm

(a)

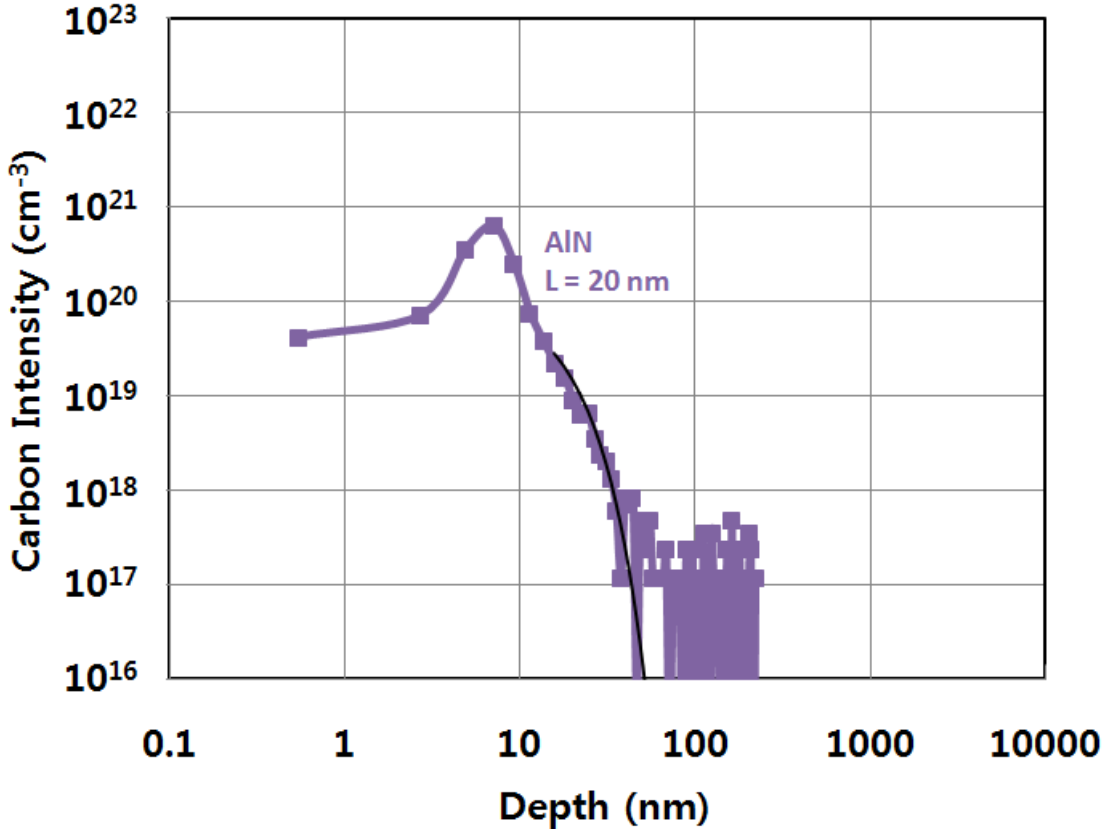
Carbon Intensity (cm-3)
10^23
10^22
10^21
10^20
10^19
10^18
10^17
10^16
0.1
1
10
100
1000
10000
Depth (nm)
AlN
L = 20 nm

(b)

Fig.1 The concentration of C along the depth of AlGaN sample (x= 0.00, 0.04, 0.45, 0.65, 1.00). (A) The C-concentration along the depth of (a) GaN, (b) deeper diffusion length of $Al_{0.04}Ga_{0.96}N$, (c) shallower diffusion length of $Al_{0.04}Ga_{0.96}N$, (d) deeper diffusion length of $Al_{0.45}Ga_{0.55}N$, (e) shallower diffusion length of $Al_{0.45}Ga_{0.55}N$, (f) deeper diffusion length of $Al_{0.65}Ga_{0.35}N$, and (g) shallower diffusion length of $Al_{0.65}Ga_{0.35}N$ sample with diffusion condition at 1000 ℃, 40 min, 100 Torr. (B) The C-concentration along the depth of AlN sample with diffusion condition at 1100 ℃, 60 min, 500 Torr.

C-concentration along the depth of $Al_xGa_{1-x}N$ (x = 0.00, 0.04, 0.45, 0.65) and AlN samples were shown in Fig. 1(a) and Fig. 1(b). These diffusion experiments were a surface diffusion plus drive-in as described by Grove [15]. The surface diffusion was represented by the complementary error function which is described by the following expression,

$$C(x,t) = C_s erfc \frac{x}{2\sqrt{Dt}} \qquad (2)$$

where x was a measured depth, t was a time, and D was diffusion coefficient, and C_s was surface concentration. The shape of experimental C-concentration along the measured depth was shown in Fig. 1(a). The diffusion length (L) of GaN, $Al_{0.04}Ga_{0.96}N$, $Al_{0.45}Ga_{0.55}N$ and $Al_{0.65}Ga_{0.35}N$ samples were 1200, 312, 250 and 250 nm, respectively, for the deeper ones, and ∞, 28, 3, 1.5 nm, respectively, for the shallower one. The diffusion length of AlN was supposed 20 nm as shown in Fig. 1(b), where $L = 2\sqrt{Dt}$. The theoretical C-concentration of $Al_xGa_{1x}N$ samples was computed by complementary error function, and it was marked as black line on the each sample in Fig. 1.

In measured depth at 200 nm, the C- concentration of GaN and $Al_{0.04}Ga_{0.96}N$ samples was about 2 x 10^{21} and 9 x 10^{19} cm^{-3}, respectively. From this result, not only the concentration of C but also the diffusion length of C was significantly changed by just 4 % of the Al

composition. The diffusion of C is severely protected by the presence of Al. Another thing is surface atoms.

$Al_{0.65}Ga_{0.35}N$ sample showed an abrupt increase of C intensity in the range of 400 nm. The concentration of C was detected as high as 2 x 10^{20} cm^{-3}. The main reason was carbon concentration along the sample depth was reached at MEE-AlN buffer layer with diffusion condition at 1000 ℃. AlN layer has very short diffusion length compare with other $Al_xGa_{1-x}N$ samples, as shown in Fig. 1(b). As a result, C atom was accumulated on the MEE- AlN buffer layer of $Al_{0.65}Ga_{0.35}N$ sample. That fact is possible to confirm as comparison of $Al_{0.04}Ga_{0.96}N$ and $Al_{0.65}Ga_{0.35}N$ samples. In Fig. 1(a), the theoretical C-concentration of $Al_{0.04}Ga_{0.96}N$, $Al_{0.45}Ga_{0.55}N$ and $Al_{0.65}Ga_{0.35}N$ samples has a names of (b) and (c), (d) and (e), and (f) and (g), respectively. The line of (b), (d) and (f) was C-concentration of $Al_{0.04}Ga_{0.96}N$, $Al_{0.45}Ga_{0.55}N$ and $Al_{0.65}Ga_{0.35}N$ samples, respectively.

But the gradient of (c), (e) and (g) lines were different from the (b), (d) and (f). Furthermore, the line of (c), (e) and (g) has almost same curvature of C-concentration. The molecular weight of Al_xC_y was heavier than C atom, therefore, Al_xC_y diffused slower than C in $Al_xGa_{1-x}N$ sample. The C-concentration line along the depth of AlGaN sample has two diffusion lengths, shallower and deeper ones. The shallower one did not calculate about the formation of Al_xC_y from Al and C atoms, we used the error function (eq. (2)) to determine the diffusion length. Also, it was possible that it was surface atoms. But, $Al_{0.04}Ga_{0.96}N$ sample with diffusion length of 16 nm reached the depth of 30 nm from the surface, as shown in Fig. 1; it is too deep as a surface atom. As a result, we predict that the (c), (e) and (g) are expected to aluminium-carbide (Al_xC_y) layer formed on $Al_xGa_{1-x}N$ or something like the surface atoms.

The diffusion coefficient of AlGaN samples was also calculated. These are shown in

Fig. 2. The diffusion coefficient of GaN, $Al_{0.04}Ga_{0.96}N$, $Al_{0.45}Ga_{0.55}N$ and $Al_{0.65}Ga_{0.35}N$ samples with diffusion condition at 1000 ℃ was estimated at 5.4 x 10^{-1}, 3.6 x 10^{-2}, 2.3 x 10^{-2} and 2.3 x 10^{-2} $\mu m^2/h$, respectively. The diffusion coefficient of AlN sample with diffusion condition at 1100 ℃ was calculated at 1 x 10^4 $\mu m^2/h$. The diffusion coefficients were sharply decreased with the existence of Al atom.

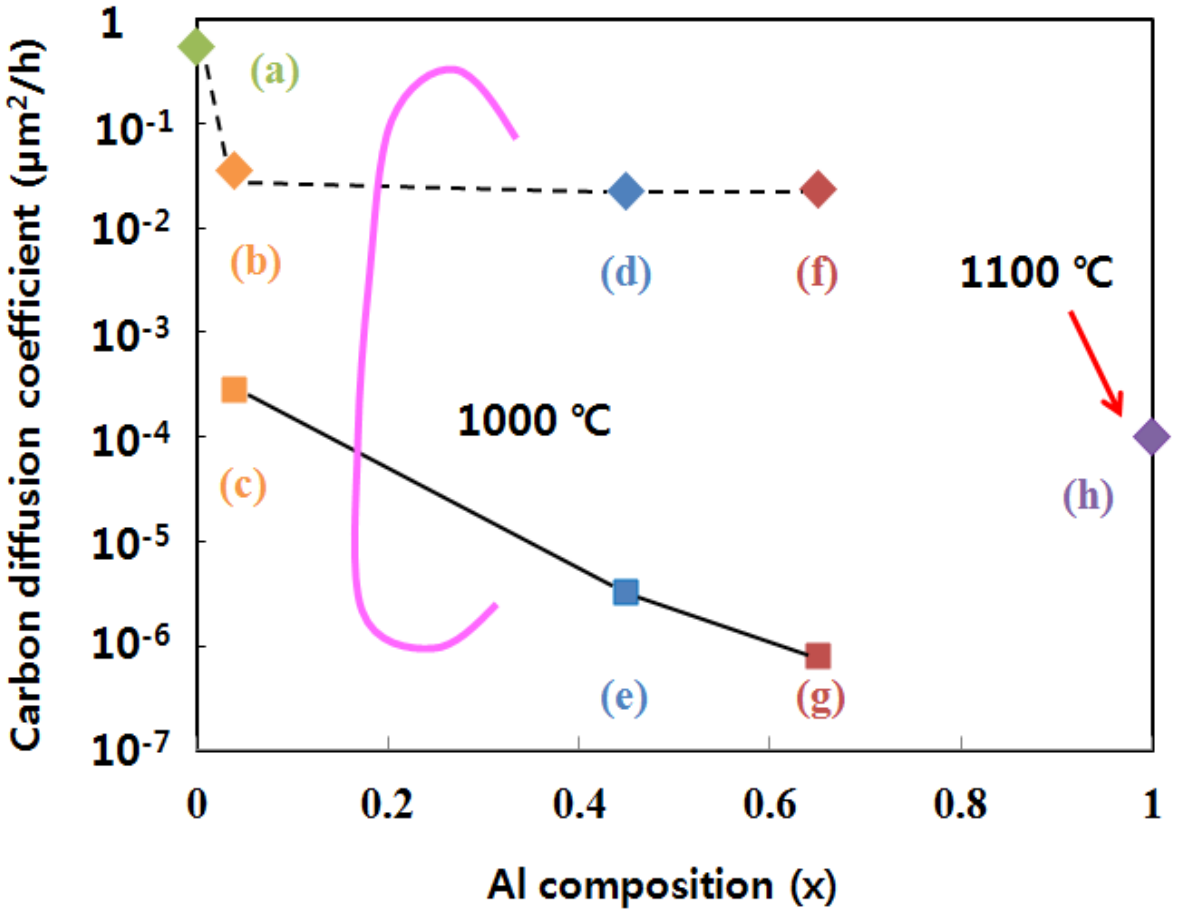

Fig.2 Carbon diffusion coefficient along the Al composition. Sample diffusion coefficient of (a) GaN, (b) deeper diffusion length of $Al_{0.04}Ga_{0.96}N$, (c) shallower diffusion length of $Al_{0.04}Ga_{0.96}N$, (d) deeper diffusion length of $Al_{0.45}Ga_{0.55}N$, (e) shallower diffusion length of $Al_{0.45}Ga_{0.55}N$, (f) deeper diffusion length of $Al_{0.65}Ga_{0.35}N$, and (g) shallower diffusion length of $Al_{0.65}Ga_{0.35}N$ sample with diffusion condition at 1000 ℃, 40 min, 100 Torr and (h) AlN with diffusion condition at 1100 ℃, 60 min, 500 Torr, respectively.

The C-concentration underneath the surface is thought to be Al_4C_3 rather than the surface atoms, because the diffusion coefficient does not significantly change with Al composition x; it is just change in the range of 10^{-4} to 10^{-7} $\mu m^2/h$. The reason of small fluctuation shown between $Al_{0.45}Ga_{0.55}N$ and $Al_{0.65}Ga_{0.35}N$ samples was speculated that the measured number is just 2 to 3 times, but diffusion coefficient of $Al_{0.04}Ga_{0.96}N$ sample for the shallower range was approximately reached to 30 nm from the surface. This suggested the possibility of Al_xC_y formed in the $Al_xGa_{1-x}N$ sample with diffusion condition at 1000 ℃.

3.5 XPS measurement

Figure 3 shows the C1s intensity of GaN, $Al_{0.45}Ga_{0.55}N$ and $Al_{0.65}Ga_{0.35}N$ samples with diffusion condition at 1000 ℃. $Al_{0.45}Ga_{0.55}N$ sample with diffusion condition at 1100 ℃ was measured to confirm the influence of diffusion condition. Al_xC_y sample was analyzed to know the C-diffusion mechanism of GaN and AlGaN sample.

C1s binding energy of GaN with diffusion condition at 1000 ℃ was detected at 282.4 eV. It is commonly found to $Al_xGa_{1-x}N$ (x = 0.45, 0.65) samples with diffusion condition at 1000 ℃ and $Al_{0.45}Ga_{0.55}N$ sample with diffusion condition at 1100 ℃. It was proven that C was diffused in GaN and AlGaN samples. It was shown that Al_xC_y was carbon diffusion material. However, C1s binding energy with 282 eV was not detected in Al_xC_y sample.

C1s binding energy with 287 eV was confirmed as Al_xC_y sample. C1s binding energy of Al_xC_y was detected to $Al_xGa_{1-x}N$ (x = 0.45, 0.65) samples with diffusion condition at 1000 ℃ and $Al_{0.45}Ga_{0.55}N$ sample with diffusion condition at 1100 ℃.

It was shown that Al_xC_y was diffused in AlGaN samples. Nevertheless, it was not observed in GaN sample with diffusion condition at 1000 ℃. In other words, constitute of Al_xC_y was not diffused in GaN sample, when the diffusion experiment was conducted. This result was same as SIMS analysis. In SIMS measurement, diffusion length of Al_xC_y was calculated in AlGaN samples, excluding GaN sample with diffusion condition at 1000 ℃. By using Hall measurement experiment, GaN sample with diffusion condition at 1000 ℃ was confirmed to n-type conduction. It was possible that the diffused Al_xC_y was changed n-type AlGaN to p-type AlGaN.

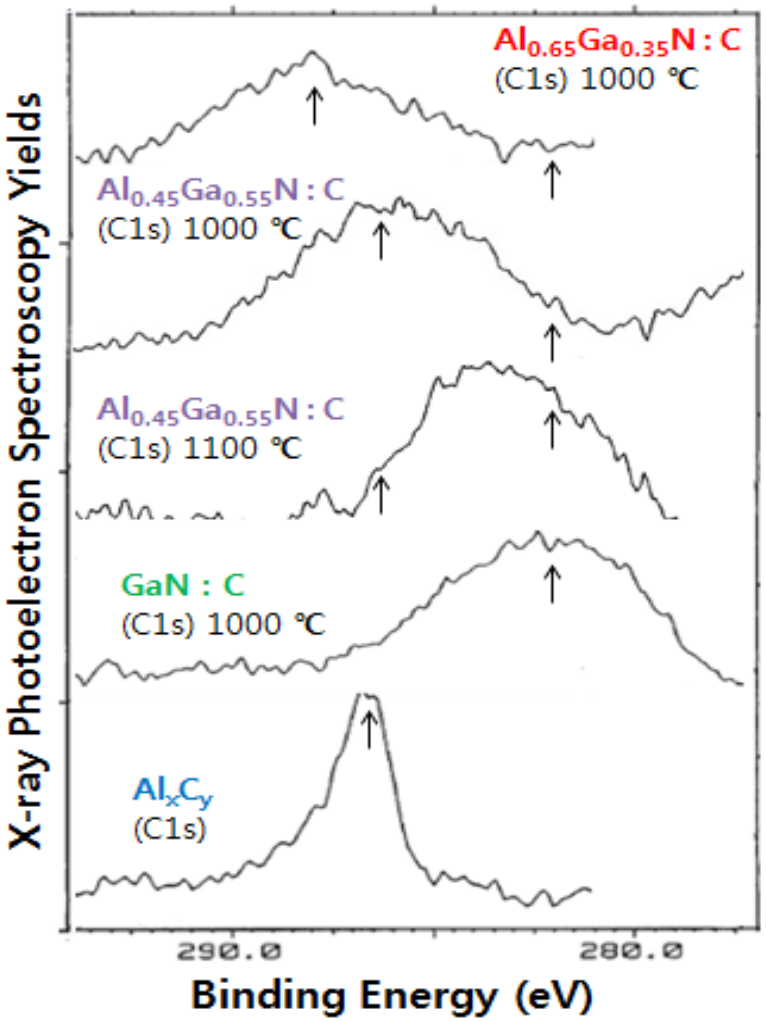

Fig.3 The C1s intensity of GaN, $Al_xGa_{1-x}N$ with diffusion experiment and Al_xC_y sample.

Figure 4 showed that the count per second of Al2p was significantly increased with increase in aluminium composition. This result was already expected. However, the increment of count per second on $Al_xGa_{1-x}N$ ($0.45 \leqq x \leqq 0.65$) was outstanding. We supposed that main reason was the sensitivity of XPS equipment.

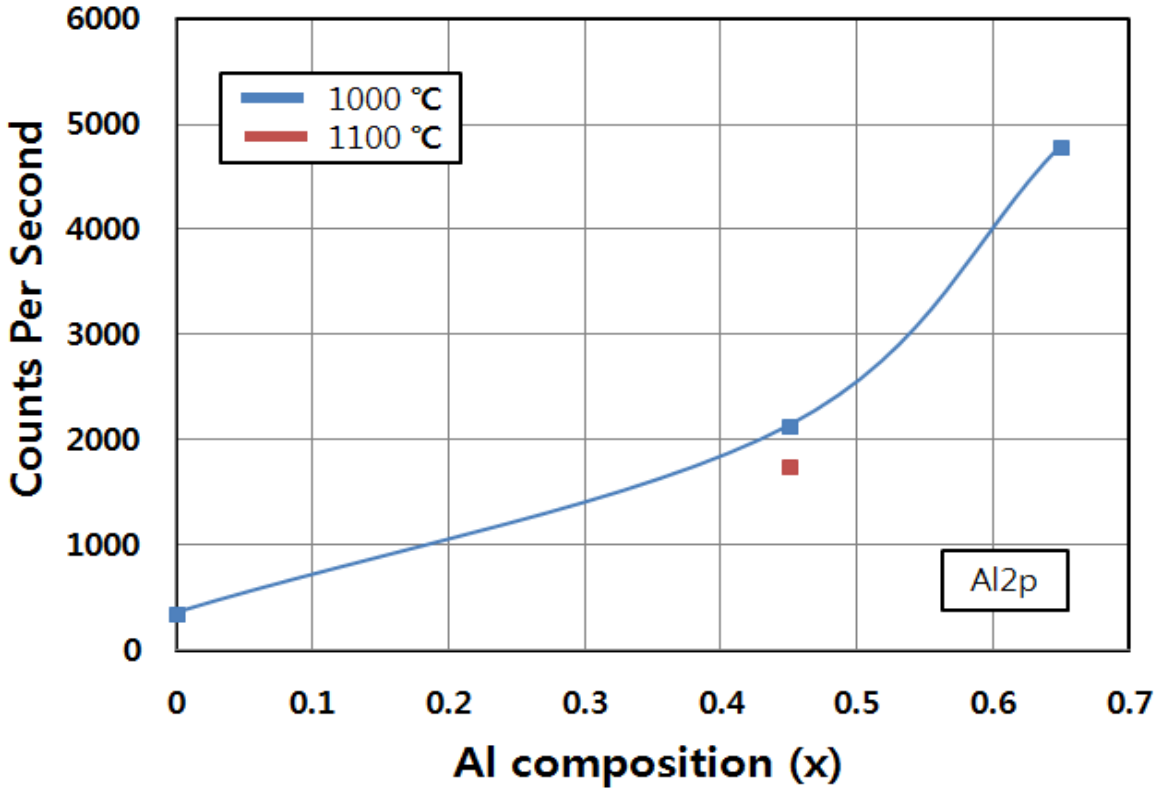

Fig.4 The count per second of Al2p along the Al composition in AlGaN sample.

Figure 5 showed that binding energy of maximum XPS yield along the Al composition in AlGaN sample. This result also showed that binding energy was significantly increased with increase in Al composition. Binding energies of GaN, $Al_{0.45}Ga_{0.55}N$ and $Al_{0.65}Ga_{0.35}N$ samples with diffusion condition at 1000 ℃ were 282.4, 285.9 and 288.5 eV, respectively. Binding energies of $Al_xGa_{1-x}N$ ($x = 0.45, 0.65$) samples with diffusion condition at 1000 ℃ were similar value with

that of Al_xC_y. Al_xC_y was diffused in $Al_xGa_{1-x}N$ sample with the higher Al composition than x = 0.45.

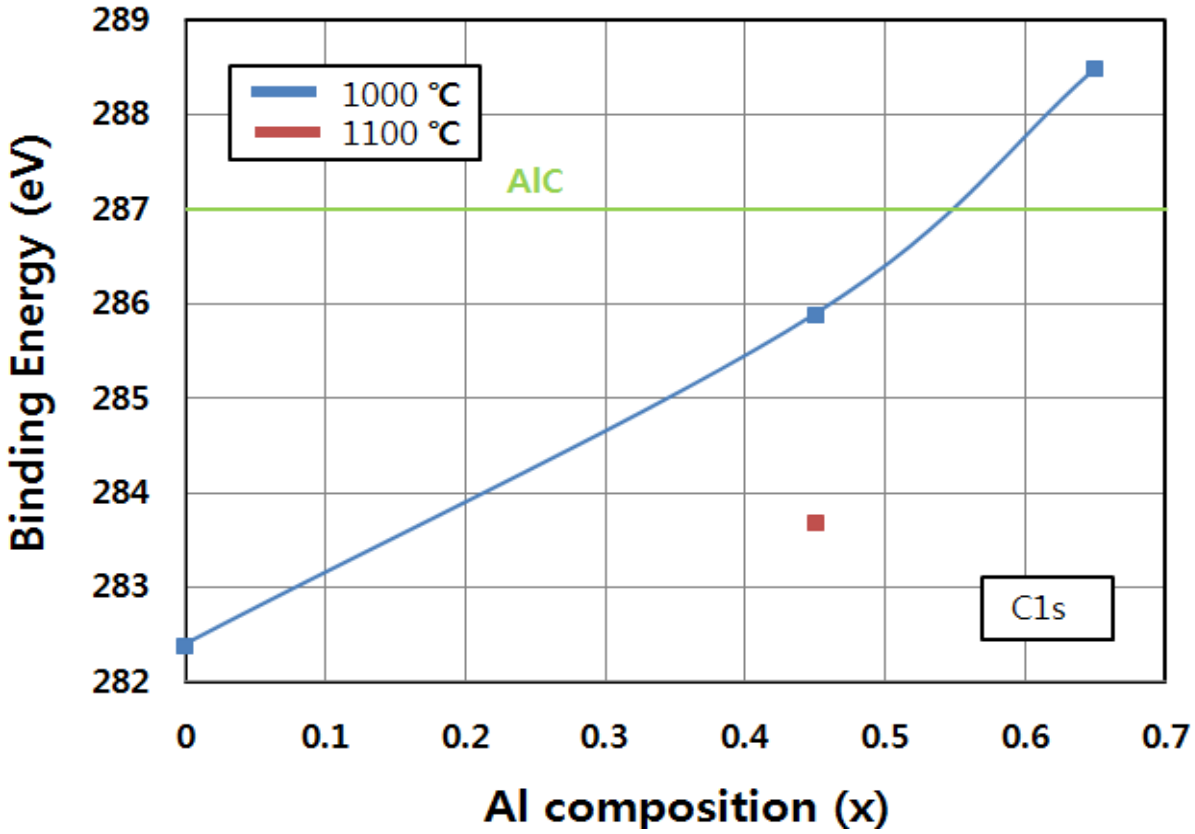

Fig.5 Binding energy of maximum XPS yield along the Al composition in AlGaN sample..

The oxidation of Al_xCy was discussed to chapter 1. Therefore, we measured XPS yields of O1s. Binding energies of maximum XPS yield in $Al_{0.45}Ga_{0.55}N$ samples With diffusion conditions at 1000 and 1100 ℃ were 535 and 532 eV, respectively. XPS yield peak of $Al_{0.45}Ga_{0.55}N$ with diffusion condition at 1000 ℃ was stronger than that of $Al_{0.45}Ga_{0.55}N$ with diffusion condition at 1100 ℃. We detected that the Al, C and O atoms were diffused in the surface of $Al_xGa_{1-x}N$ by the oxidized Al_xC_y.

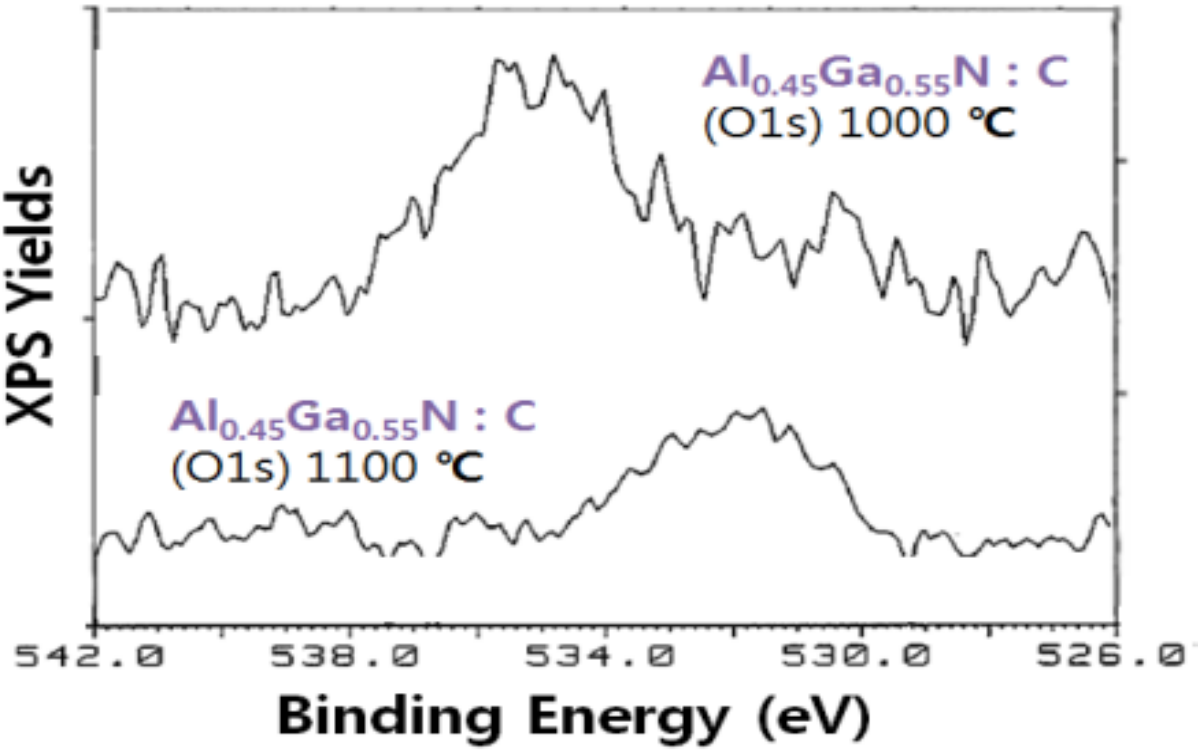

Fig.6 Binding energy of O1s on AlxGa1-xN with diffusion condition at 1000 and 1100 ℃.

Figure 7 showed that XPS areas along the various atoms of $Al_{0.45}Ga_{055}N$ samples with diffusion conditions at 1000 and 1100 ℃. XPS areas of C1s and Al2p in $Al_{0.45}Ga_{0.55}N$ with diffusion conditions at 1000 and 1100 ℃ were gradually decreased with increase in depth from the surface. In contrast, XPS areas of Ga 3p1/s2p and O1s in $Al_{0.45}Ga_{0.55}N$ with diffusion conditions at 1000 and 1100 ℃ were different. Although measured depth was increased in sample, XPS areas were not decreased. This phenomenon was especially notable to Ga 3p1/s2p. High XPS areas of AlGaN surface was proven that Al and C atoms of the decomposed Al_xC_y was diffused in AlGaN.

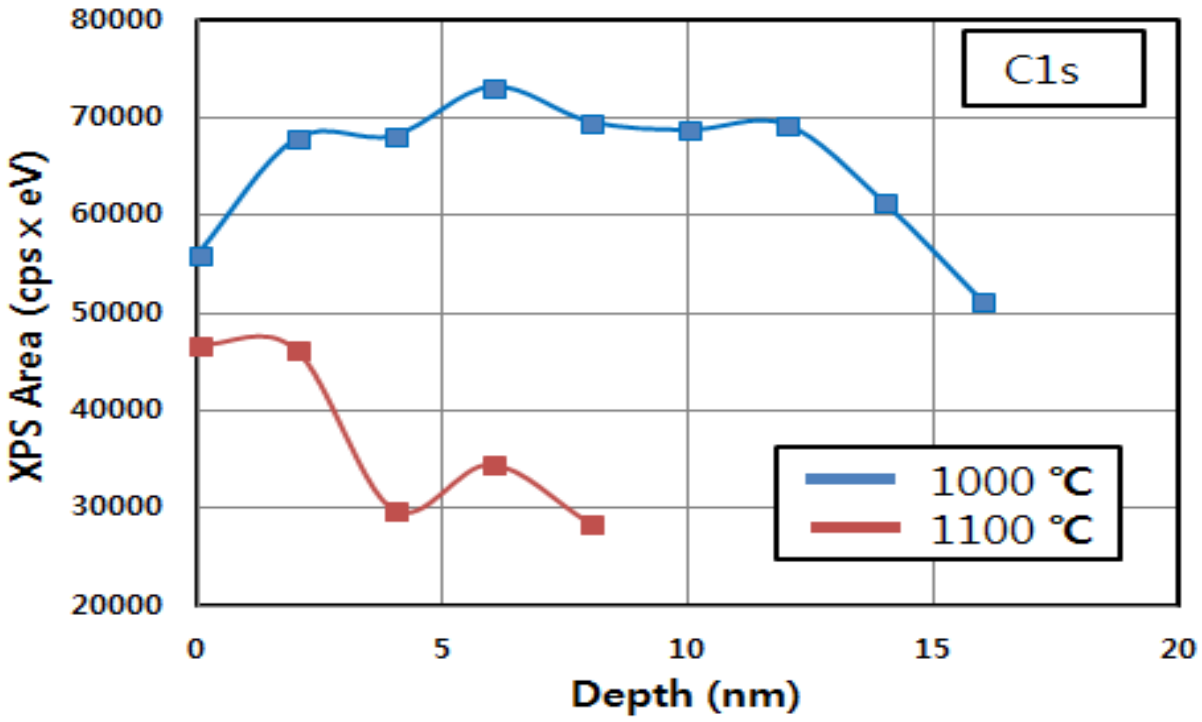

Fig.7 (a) C1s intensity of $Al_{0.45}Ga_{0.55}N$ with diffusion condition at 1000 and 1100 ℃.

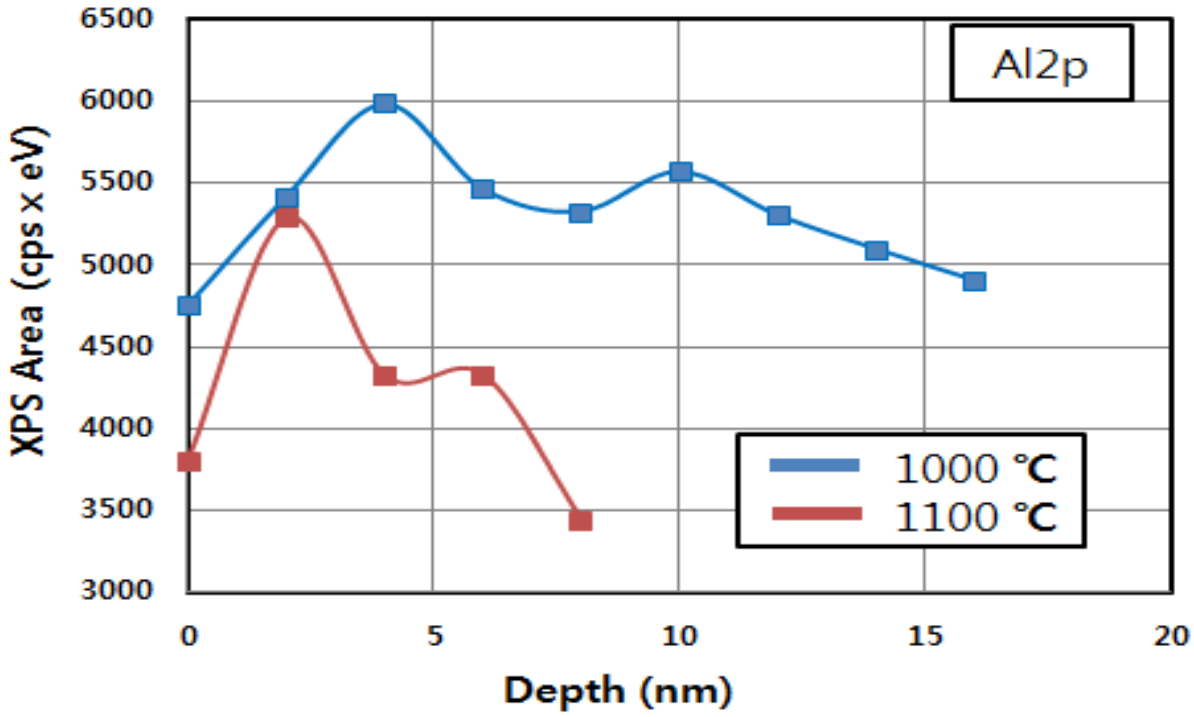

Fig.7 (b) Al2p intensity of $Al_{0.45}Ga_{0.55}N$ with diffusion condition at 1000 and 1100 ℃.

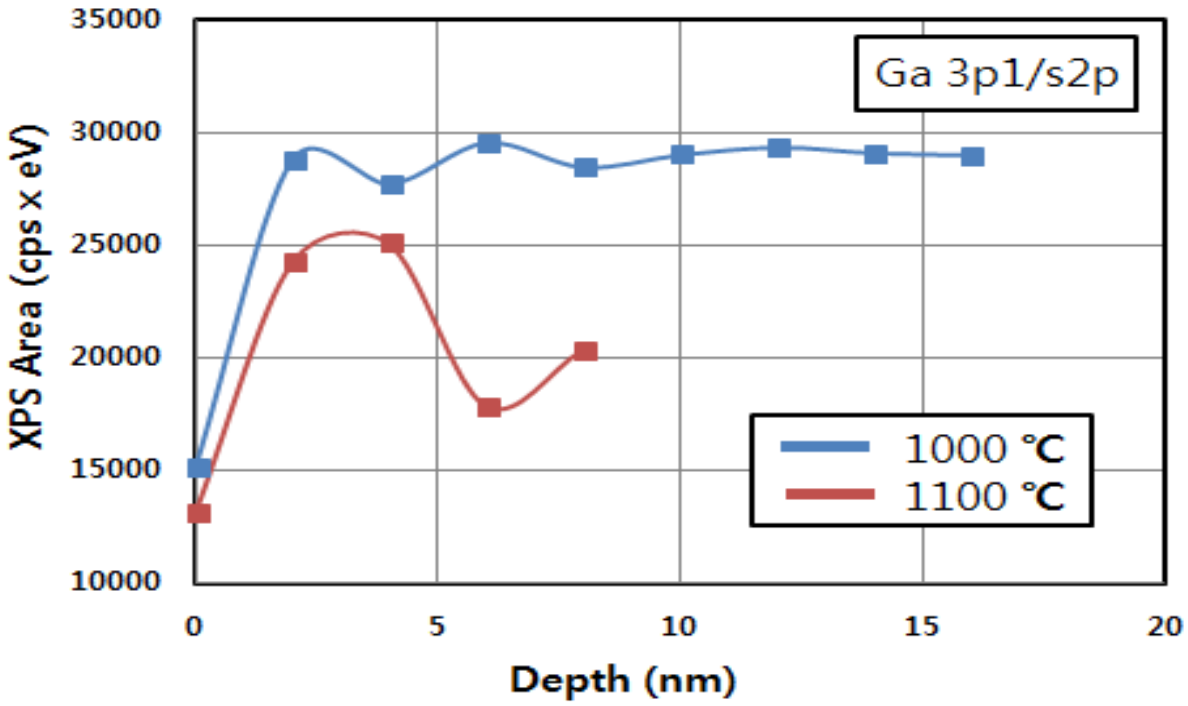

Fig.7 (c) Ga 3p1/s2p intensity of $Al_{0.45}Ga_{0.55}N$ with diffusion condition at 1000 and 1100 ℃.

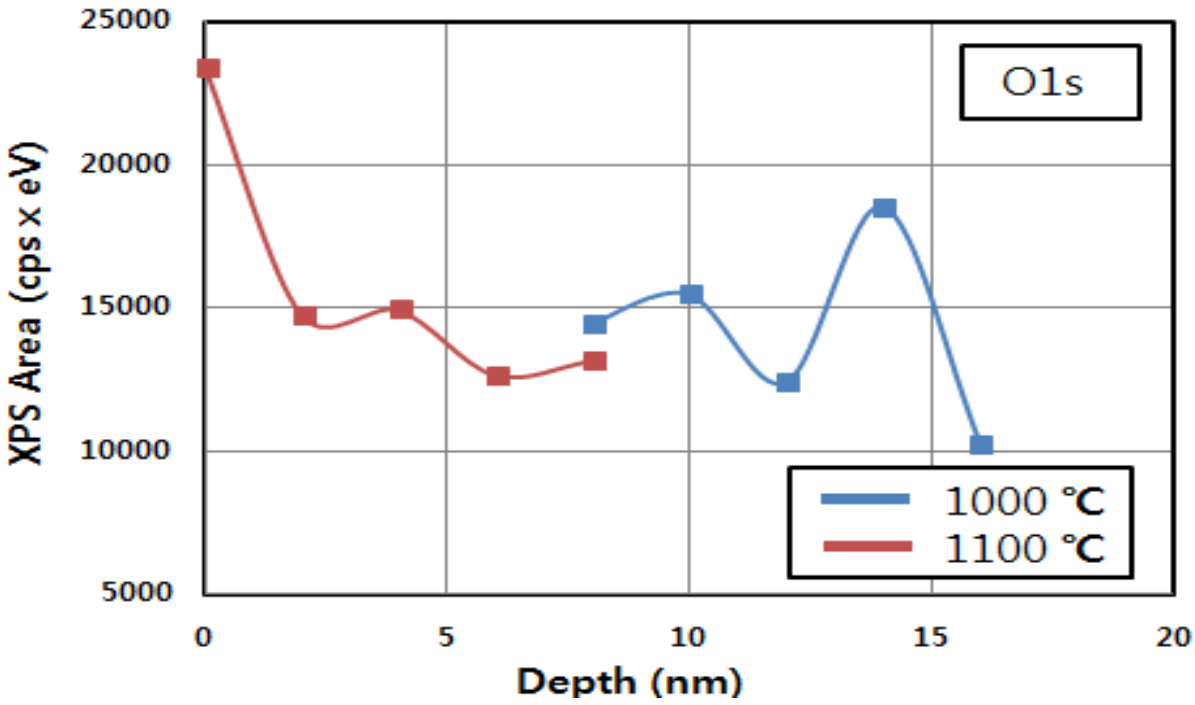

Fig.7 (d) O1s intensity of $Al_{0.45}Ga_{0.55}N$ with diffusion condition at 1000 and 1100 ℃.

3.5 Summary

We performed a p-type $Al_xGa_{1-x}N$ using by Al_xC_y diffusion method, and calculated these diffusion coefficients. The conductivity of n-type $Al_xGa_{1-x}N$ ($x \leqq 0.45$) samples was changed to p-type conduction after the diffusion experiment at 1000 ℃.

The C-concentration, the diffusion length and the coefficient of C were rapidly decreased by the existence of Al composition. In diffusion condition at 1000 ℃, the diffusion coefficients of GaN, $Al_{0.04}Ga_{0.96}N$, $Al_{0.45}Ga_{0.55}N$, $Al_{0.65}Ga_{0.35}N$ samples were at 5.4×10^{-1}, 3.6×10^{-2}, 2.3×10^{-2} and 2.3×10^{-2} $\mu m^2/h$, respectively. In diffusion condition of 1100 ℃, the diffusion coefficient of AlN sample was calculated at 1×10^{-4} $\mu m^2/h$.

Al_xC_y binding energy of $Al_{0.45}Ga_{0.65}N$ sample with diffusion condition at 1000 and 1100 ℃ and $Al_{0.65}Ga_{0.35}N$ with diffusion condition at 1000 ℃ was detected. However, it was not observed at GaN sample with diffusion condition at 1000 ℃. It is possible that Al_xC_y affect the formation mechanism of p-type AlGaN. Also, it was confirmed that Al, C and O atoms of Al_xC_y were simultaneously diffused in surface of AlGaN sample.

Reference

[1] H. Sato, H. Wang, D. Sato, R. Takaki, N. Wada, T. Tanahashi, K. Yamashita, S. Kawano, T. Mizobuchi, A. Dempo, K. Morioka, M. Kimura, S. Nohda, T. Sugahara and S. Sakai: Phys. Status Solidi A. **200** (2003) 102.

[2] C. Pernot, M. Kim, S. Fukahori, T. Inazu, T. Fujita, Y. Nagasawa, A. Hirano, M. Ippommatsu, M. Iwaya, S. Kamiyama, I. Akasaki and H. Amano: Appl. Phys. Express **3** (2010) 061004.

[3] H. Amano, M. Iwaya, N. Hayashi, T. Kashima, S. Nitta, C. Wetzel, and I. Akasaki, Phys stat sol (b). 216 (1999) 683.

[4] M. Katsuragawa, S. Sota, M. Komori, C. Anbe, T. Takeuchi, H. Sakai, H. Amano and I. Akasaki: J. Cryst. Growth 189/190 (1998) 528.

[5] J. L. Lyons, A. Janotti and C. G. Van de walle: Appl. Phys. Lett. **97** (2010) 152108.

[6] P. Bogustawski and J. Bernholc: Phys. Rev. B, **56** (1997) 9496.

[7] A. F. Wright: J. Appl. Phys, **92** (2002) 2575.

[8] D. S. Green, U. K. Mishra and J. S. Speck: J. Appl. Phys. **95** (2004) 8456.

[9] N. Koide, T. Hikosaka, Y. Honda, M. Yamaguchi and N. Sawaki: J. Appl. Phys. **45** (2006) 7655.

[10] H. Kawanishi and T. Tomizawa: Phys. Status Solidi B. **249** (2012) 459.

[11] F. Horie, Y. Ohnishi, Y. Naoi and S. Sakai: Ext. Abstr. (30st Summer Meet., 2011) ; Elctronic Materials Symposium, Th2-16.

[12] D. Kim, H. Lee, K. Yamazumi, Y. Naoi and S. Sakai: Ext. Abstr. (73rd Summer Meet., 2012); Japan Society of Applied Physics and Related Societies, 12p-H9-15.

[13] R. G. Banal, M. Funato and Y. Kawakmi: Phys. Status Solidi C. **7** (2010) 2111.

[14] B. Arnaudov, T. Paskova, S. Evtimova, E. Valcheva, M. Heuken and B. Monemar: Phys. Rev. B **67** (2003) 045314.

[15] S. Nakamura and G. Fasol: *The Blue Laser Diode* (Springer, New York, 1997), p.113.

[16] A. S. Grove: *Physics and Technology of Semiconductor Devices* (Wiley, New York, 1967), p. 43.

Chapter 4

Light-Emitting Diodes with C-doped AlGaN layer by the insertion of Al_4C_3

4.1 Introduction

The characteristics of Al_4C_3 grown by metalorganic vapor phase epitaxy (MOVPE) were reported in chapter 2 [1-5]. In chapter 3, the diffusion experiment in AlGaN was shown by using the Al_4C_3.

Based on the result of chapter 2 and 3, carbon (C)-doped AlGaInN LED was fabricated by using the vaporized Al_4C_3 in this chapter. The electrical and optical charact eristics of C- and magnesium (Mg)-doped AlGaInN LED were reported [6].

4.2 Hall measurement of C-doped $Al_{0.20}Ga_{0.80}N$

4.2.1 Experimental procedure

The growth experiment was started by doping AlGaN, as shown in Fig. 1. A 2 inch Al_2O_3 (0001) wafer was chemically cleaned. H_2 annealing of 1150 ℃ was performed for 10 min by MOVPE. Then, Al_4C_3/Al_2O_3 (0001) sample with a size of 1 x 1 mm^2 was placed at the center of 2 inch sapphire substrate.

The growth procedure was started with the growth of buffer-GaN layer. The flow rates of NH_3 and TMGa were 142.8 mmol/min and 43.6 μmol/min. The growth temperature and pressure were 450 ℃ and 500 Torr. After then, undoped $Al_{0.20}Ga_{0.80}N$ layer was grown. The flow rate of NH_3 was same buffer-GaN layer. The flow rates of trimethlygallium (TMGa) and trimethylaluminum (TMA) were 43.6-87.2 μmol/min and 10.1–15.2 μmol/min. The growth temperature, pressure and time were a high temperature 1000℃, 100 Torr and 60 min, respectively.

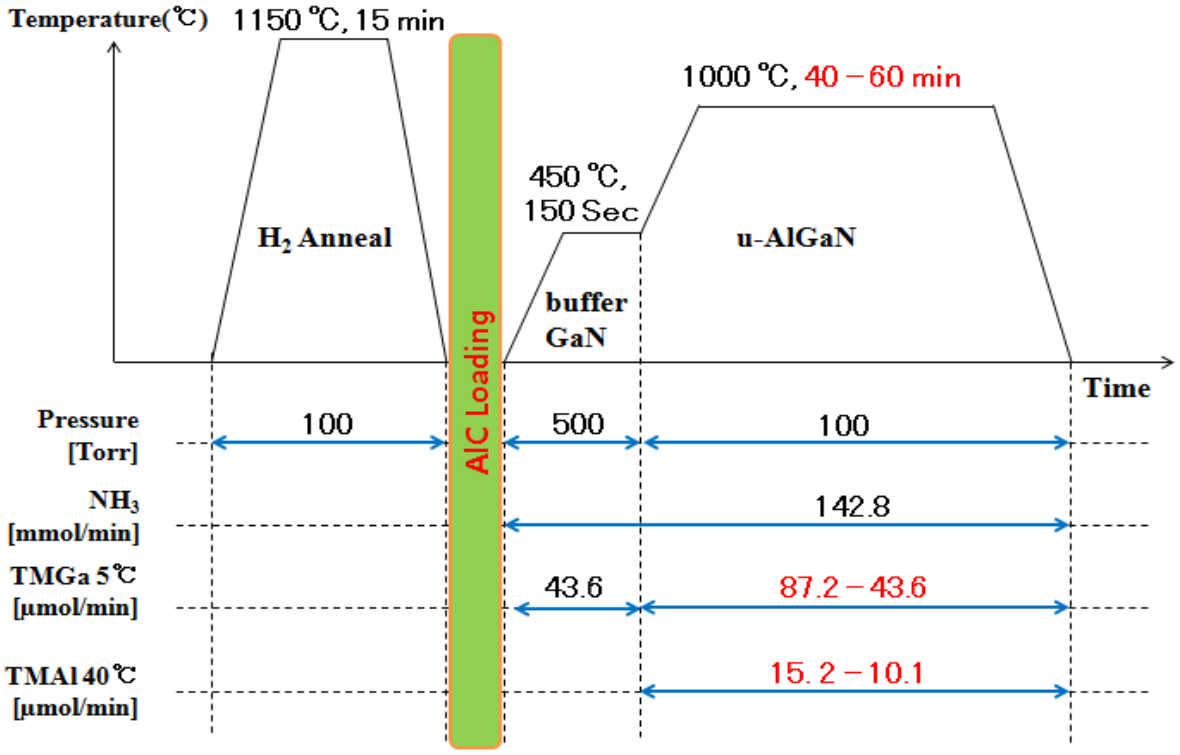

Fig. 1. The growth condition of C-doped $Al_{0.20}Ga_{0.80}N$ sample.

C-doped $Al_{0.20}Ga_{0.80}N$ samples consisted of a 300-Å GaN buffer layer and a 1.2-μm-thick undoped $Al_{0.20}Ga_{0.80}N$ layer. Figure 2(a) shows the grown sample. During growth step, Al_4C_3/Al_2O_3 (0001) was positioned at the black zone of the center. Then, the 2 inch grown sample was cut to obtain each (1, 2, 3, 4, 5).

Figure 2(b) schematically shows all the points (1, 2, 3, 4, 5). Each sample was classified by the distance of Al_4C_3/A_2O_3 (0001). To verify p- or n-type conduction, van der Pauw method was implemented. The electrode of Ni/Au was deposited by electron beam evaporation. The thickness of Ni and Au were 10 and 10 nm, respectively. Annealing was conducted in N_2 atmosphere at 520 ℃ for 10 min.

Afterward, Hall measurement was performed at RT. Constant magnetic intensity (1000 G) and current (1 mA) were used for experiment.

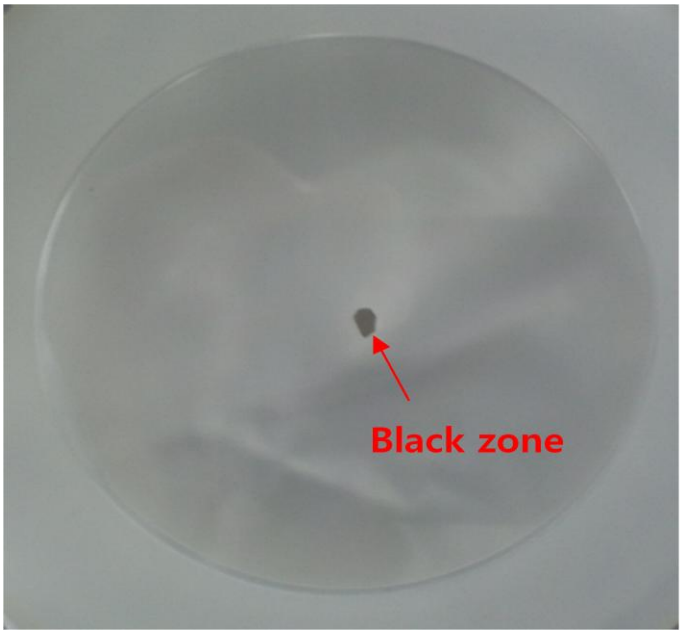

(a)

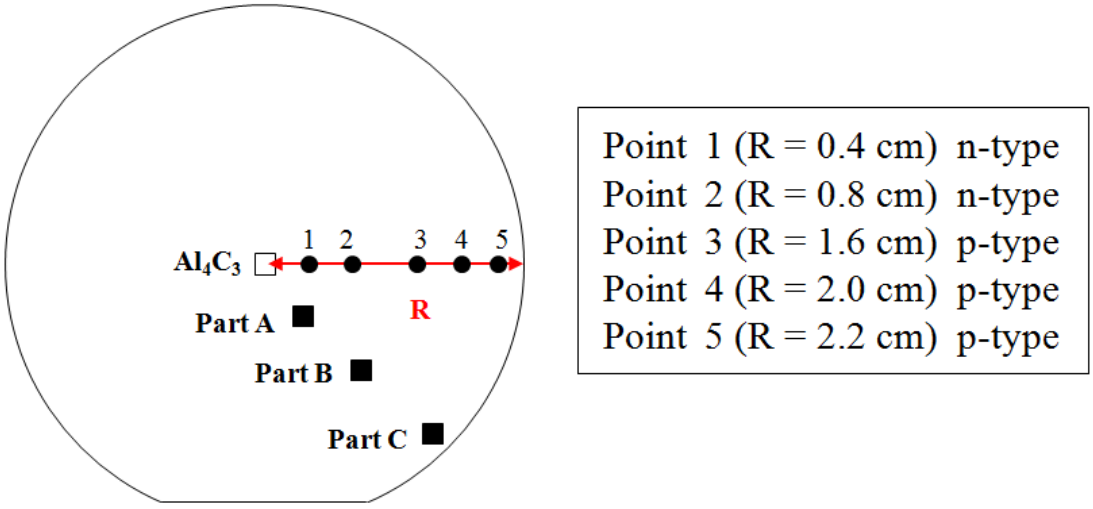

(b)

Fig.2 (a) Microscopy image of p-AlGaN doped with Al_4C_3. (b) The Hall effect result of p- or n-type conduction of $Al_{0.20}Ga_{0.80}N$ sample along each point (1, 2, 3, 4, 5). Parts A, B, and C used in the SIMS analysis.

4.2.2 Result and discussion

The characteristics of n- or p-type conduction in each $Al_{0.20}Ga_{0.80}N$ sample was shown in Fig. 2(b). Conduction of n-type was observed at point 1 and 2. On the other hands, point 3, 4, and 5 were p-type. Electron concentrations of parts 1 and 2 were 4 x 10^{16} and 3 x 10^{16} cm^{-3}, respectively. Hole concentrations of parts 3, 4, and 5 were 1.9 x 10^{18}, 8.8 x 10^{17}, and 1.7 x 10^{17} cm^{-3}, respectively. Figure 3 shows electron and hole concentration of points (1, 2, 3, 4, 5).

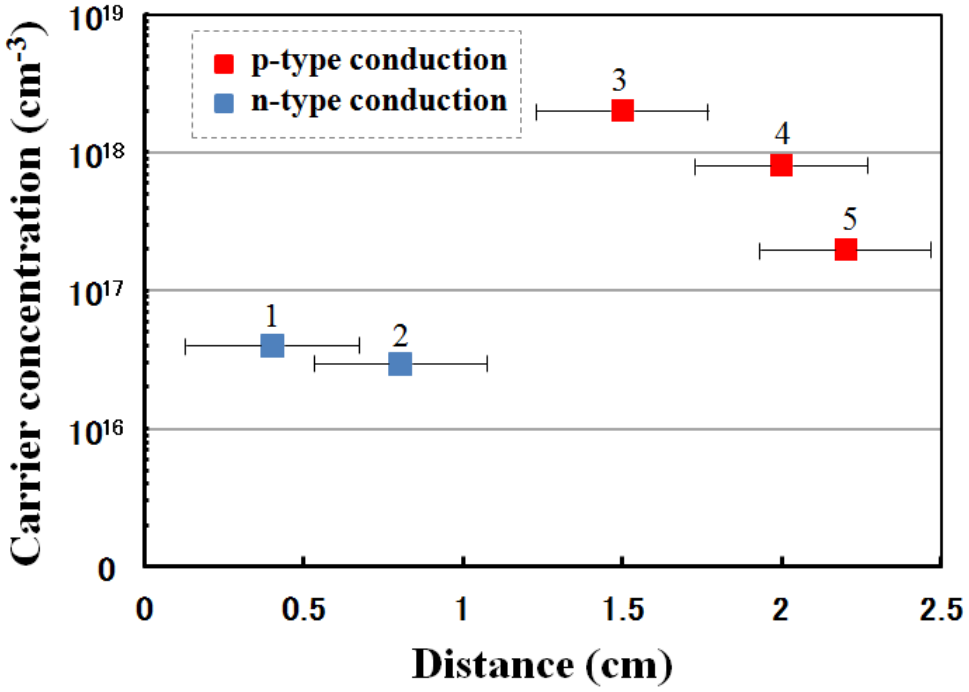

Fig.3 Electron and hole concentrations of C-doped $Al_{0.20}Ga_{0.80}N$ sample along each point (1, 2, 3, 4, 5).

The mobility of points 3, 4, and 5 were higher than 200 $cm^2/(V.s)$. This hole mobility is large value. The main reason is coexistence of n- and p-type. Al_4C_3 was decomposed in this growth procedure. P-type conduction was assumed to

occur in the early growth stage and n-type conduction was assumed after near the surface. In other words, u-$Al_{0.20}Ga_{0.80}N$ existed in p-$Al_{0.20}Ga_{0.80}N$. As a result, the mob ility of this sample should be apply the effect of u- and p-$Al_{0.20}Ga_{0.80}N$ layers.

A multilayer model for Hall effect data analysis was used to calculate the p-$Al_{0.20}Ga_{0.80}N$ mobility and concentration [7]. This sample is a partially connected two-layer structure. This cases, the two n- and a single p-layers are connected and voltage applied to the Hall effect is higher than the band-gap energy divided by an electric charge. To apply this system, assumed mobility and depth of n-$Al_{0.20}Ga_{0.80}N$ are 291 $cm^2/(V.s)$ and 0.1 µm, respectively. p-$Al_{0.20}Ga_{0.80}N$ is 1.1 µm. Calculated hole concentration and mobility were 1.08 x 10^{18} cm^{-3} and 8 $cm^2/(V.s)$. It showed in Fig. 4. The experimental results correspond with the observation of both n- and p-type conductions.

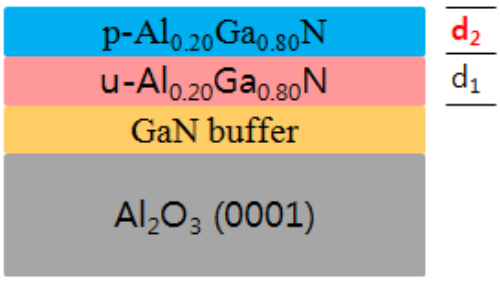

$$n_2 = \frac{1}{d_2}\frac{(\mu^* n^* d - \mu_1 n_1 d_1 t_1)^2}{\mu^{*2} n^* d - \mu_1^2 n_1 d_1 t_1^2}$$

$$\mu_2 = \frac{\mu^{*2} n^* d - \mu_1^2 n_1 d_1 t_1^2}{\mu^* n^* d - \mu_1 n_1 d_1 t_1}$$

Al composition (x) of $Al_xGa_{1-x}N$	d (µm)	n, p (Cm^{-3})	μ_n, μ_p ($Cm^{-3}/V{\cdot}S$)	ρ (Ω·C m)
0.20	d_2= 1.1	p=1.0x10^{18}	μ_p=8	0.77
	d_1= 0.1	n=3.0x10^{17}	μ_n=291	0.07

Fig.4 Electron and hole concentrations of C-doped $Al_{0.20}Ga_{0.80}N$ sample by a multilayer model for Hall effect data analysis [7].

4.3 C-doped AlGaInN LED

4.3.1 Experimental procedures

Al_2O_3 (0001) substrate of a diameter 2 inch was chemically cleaned. All III-V nitride layers were grown by MOVPE method. TMGa, TMA, and trimethylindium (TMIn) were used as group III sources, and NH_3 was used as group V source. Hydrogen (H_2) and nitrogen (N_2) were used as sub flow gases. Aluminium carbide (Al_4C_3), Biscyclo-pentadienyl magnesium (Cp_2Mg) and Silane (SiH_4) were used as the p- , p- and n-type doping materials, respectively.

The Al_4C_3/Al_2O_3 (0001) was placed on the center of the 2-in Al_2O_3 (0001) wafer that was already H_2-annealed at 1150 ℃. This method was same manner as the p-$Al_{0.20}Ga_{0.80}N$ sample. Ammonia (NH_3) flow rate was 3.2 SLM. The growth was conducted at low pressure MOVPE (LP-MOVPE), and the suceptor was rotated. The growth condition was shown in Fig. 5.

The structure of AlGaInN LED device was shown in Fig. 6. The sample was consisted of a 30 nm GaN buffer layer grown at a low temperature of 450℃, a 1.8-μm-thick-layer-undoped GaN, a 2.73-μm-thick n-type GaN:Si, 25 strained super lattice (SLs) of a n-type $Al_{0.18}Ga_{0.82}N$:Si (15-Å)/n-type GaN:Si (15-Å), 3 periods of a u-GaN (40-Å)/ $In_{0.05}Ga_{0.95}N$ (13-Å) MQW structure, 10 periods of a u-$Al_{0.19}Ga_{0.81}N$ (15-Å)/ p-type GaN:Mg (15-Å), and a 38-Å -thick layer of p-type GaN:Mg. A Mg- doped AlGaInN LED structure was just grown on Al_2O_3 (0001) without Al_4C_3/Al_2O_3 (0001) source. Mg-doped AlGaInN LED structure with p-type $Al_{0.19}Ga_{0.81}N$:Mg layer was grown at same growth manner to compare it with C-doped AlGaInN LED. The growth temperatures were 980, 930, and 950 ℃ for (undoped GaN, Si-doped GaN, Si-SLS), MQW and p-type layers, respectively.

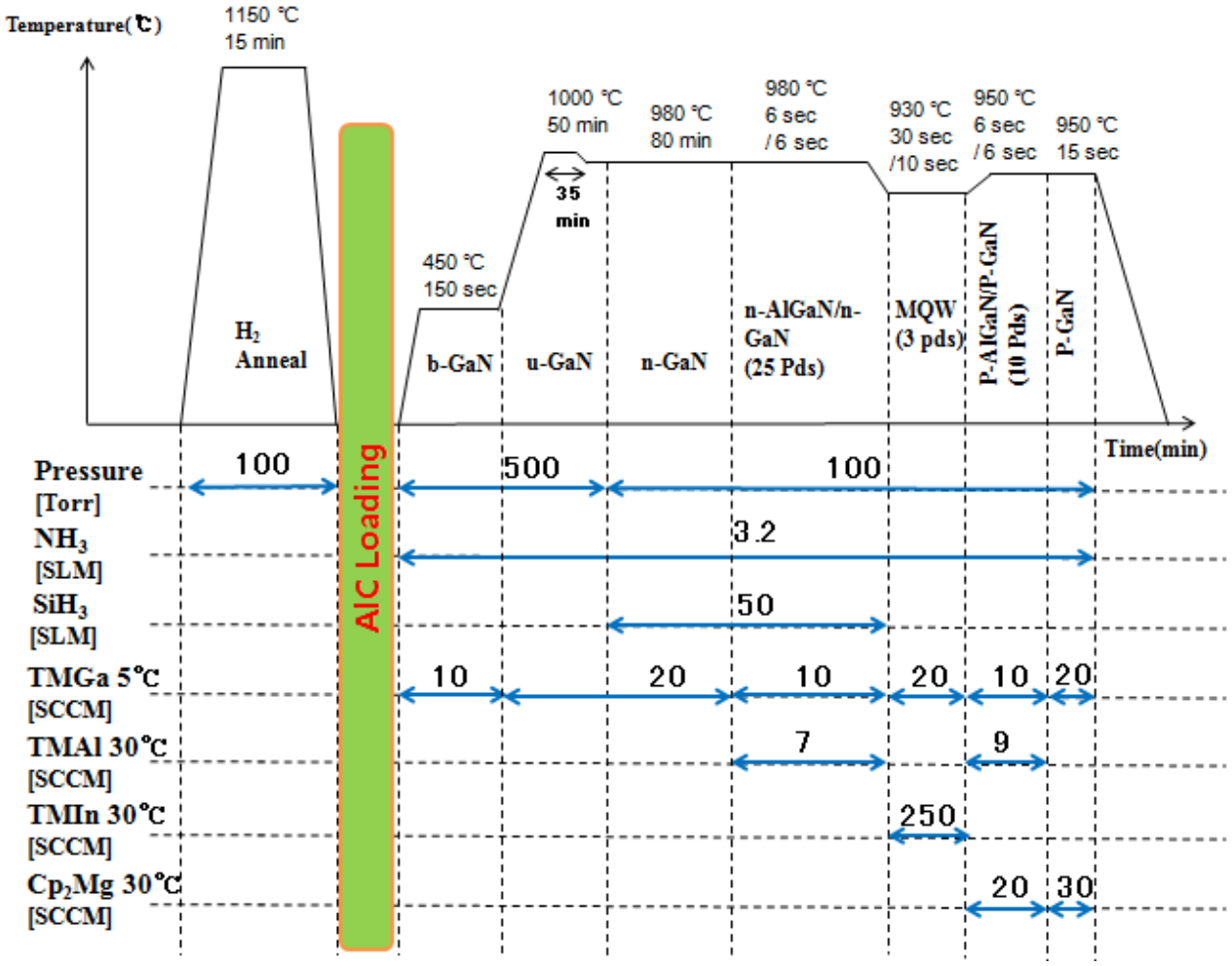

Fig.5 The growth condition of C-doped AlGaInN LED sample.

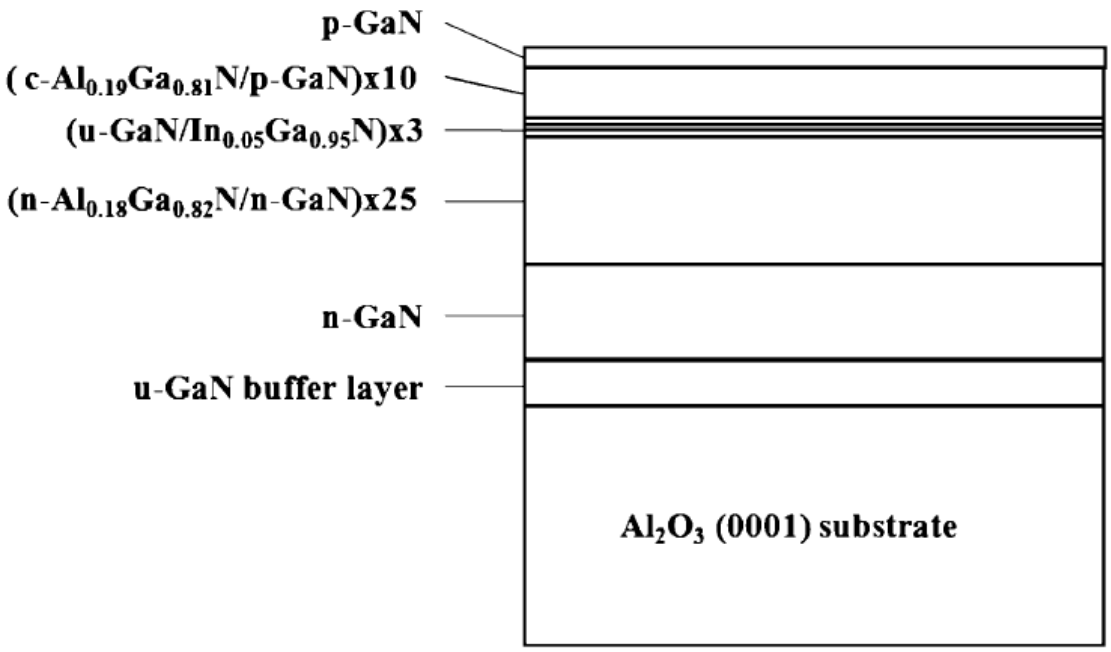

Fig.6 Structure of AlGaInN based LED.

After then, C- and Mg-doped AlGaInN LED samples were cut into six pieces to show the another experiment. One C-doped AlGaInN LED and Mg-doped AlGaInN LED were annealed in N_2 atmosphere at 800℃ for 20 min to activate p-type GaN. Detailed process of AlGaInN LED chip was shown in Fig. 7.

We distinguished the grown C-doped AlGaInN LED chips at the radius (R) of a 2 inch size sample. The sample designated part A, B, and C. The R (cm) of parts A, B, and C were $0 \leqq R \leqq 0.5$, $0.5 \leqq R \leqq 1.5$, and $1.5 \leqq R \leqq 2.5$, respectively.

We called parts A, B, and C as the center, the half of center and edge, and the edge, respectively.

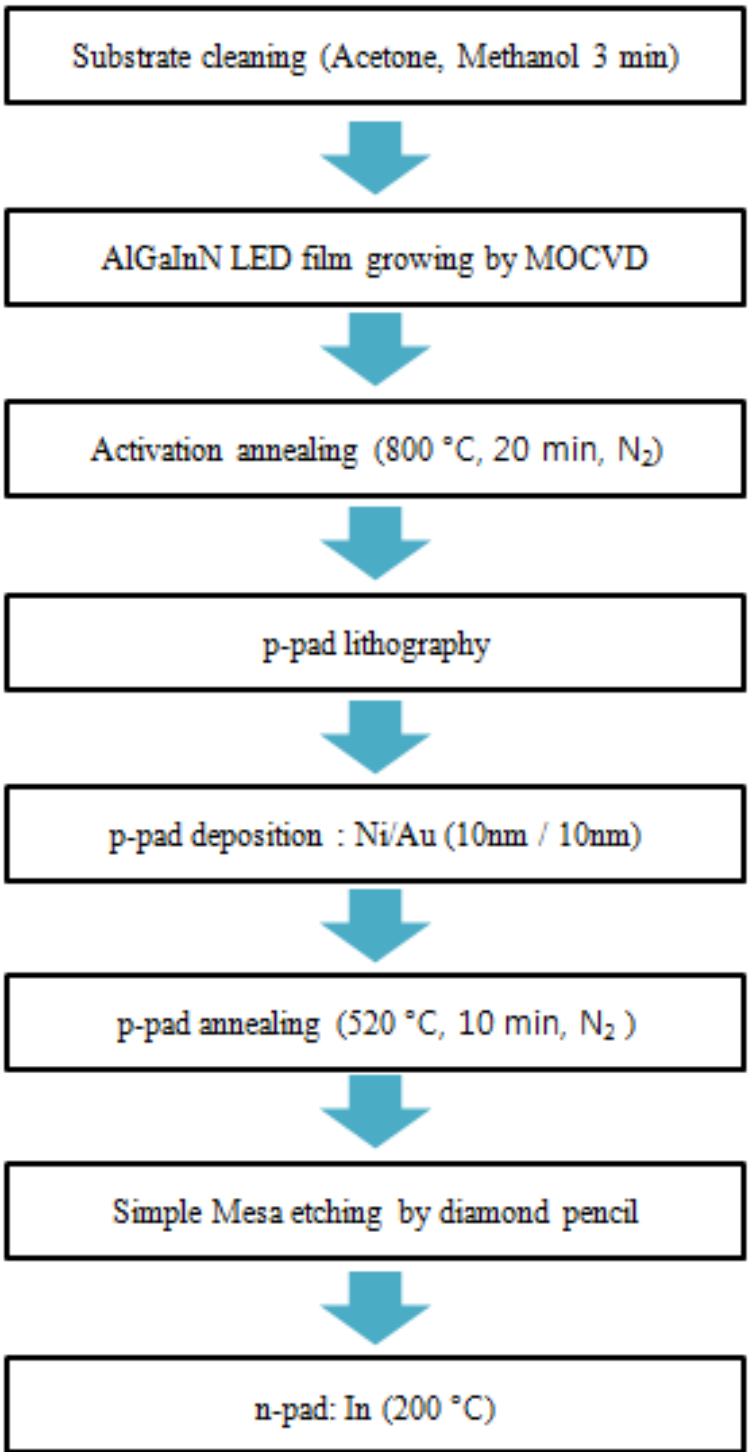

Fig.7 Flow chart of the AlGaInN LED chip process.

4.3.2 Result and discussion

Figure 8 showed cross-sectional scanning electron microscope (SEM) image of C-doped AlGaInN LED. The cross-sectional thickness of C-doped AlGaInN LED was detected 5.4 μm. This result was almost consistent with expected thickness.

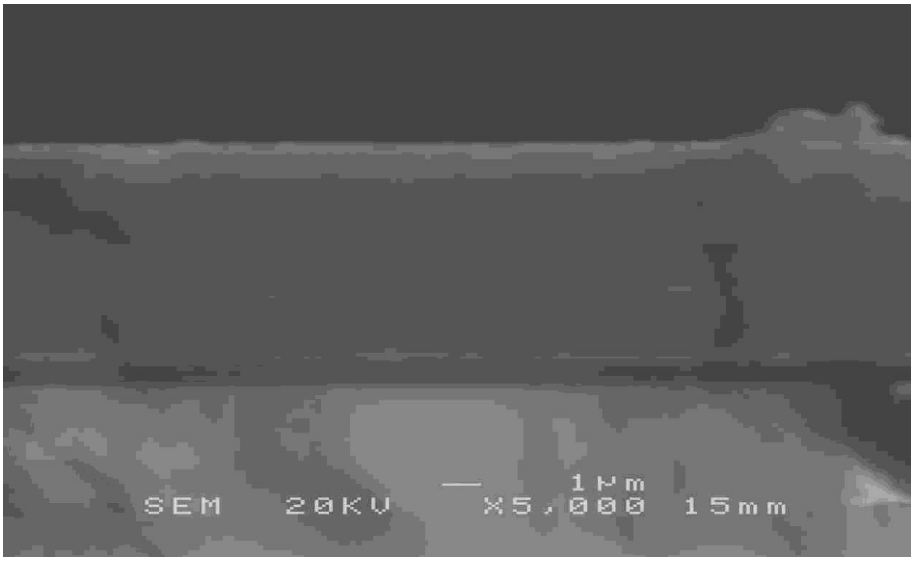

Fig.8 The cross-sectional SEM image of C-doped AlGaInN LED sample.

Figure 9 shows C and Si concentrations of C-doped AlGaInN LED sample along the distance from Al_4C_3 placed on the 2" Al_2O_3 (0001) wafer. The C concentration of Part A (center) had a low value of 10^{17} cm^{-3}, as shown in Fig. 9(a). It showed that Part A was not doped with C. On the contrary, the Si concentration in the range of 10^{17} to 10^{18} cm^{-3} was observed at a depth of 100 nm and abruptly increased to a value higher than 10^{19} cm^{-3} at a deeper depth. We did not expect to grow the pn junction structure LED.

The C concentration of Part B (half of center and edge) was a 10^{17} cm^{-3}, as shown in Fig. 9(b). It showed that C concentration of Part B was a little bit higher than that in Part A, but it did not exceed 10^{18} cm^{-3}. Therefore, we assumed that this Part B was not effectively doped with C. The Si concentration was higher value than 10^{19} cm^{-3}

at all depths of sample. The main reason was Si was additionally supplied to the LED growth experiment from Al_4C_3/Al_2O_3 (0001). When the SiH_4 supply was flowed in the LED growth step, SiH_4 was also supplied on Al_4C_3 layer. Although SiH_4 supply was stopped in this process, Al_4C_3 with Si atoms was kept providing Si atoms by decomposition of the layer. As a result, Si concentration was kept in the 10^{19} cm^{-3}. This again indicates that the pn junction LED was not grown.

The C concentration of Part C was a higher than 10^{18} cm^3 at a depth shallower than 50 nm and decreased with increasing with depth, as shown in Fig. 9(c). Al_4C_3 with carbon atom was decomposed and flowed into the layer in the growth procedure. Concentration of Si was showed similar tendency of Fig. 9(a). It also showed abrupt Si concentration at a larger depth. It implied that Part C had faster gas flow and that the pn junction LED was fabricated.

C-doped AlGaInN LED structure manufactured by the insertion of Al_4C_3 was attained in Part C (edge) by the result of SIMS analysis. The reason was that C concentration in the range of 10^{18} cm^{-3} was analyzed at a depth of 30 nm. Also, Si concentration higher than 10^{18} cm^{-3} was detected at a depth of 100 nm. This result shows that the pn junction was formed in the area of Part C.

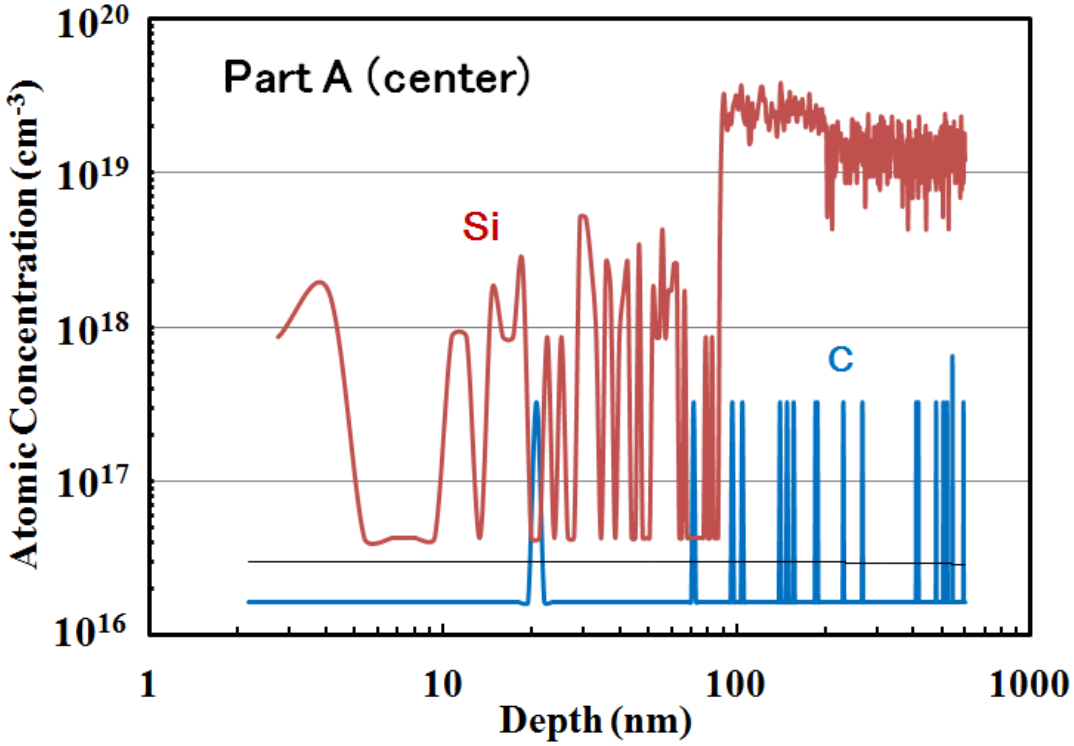

Fig. 9(a) Concentrations of C and Si in Part A of C-doped AlGaInN LED.

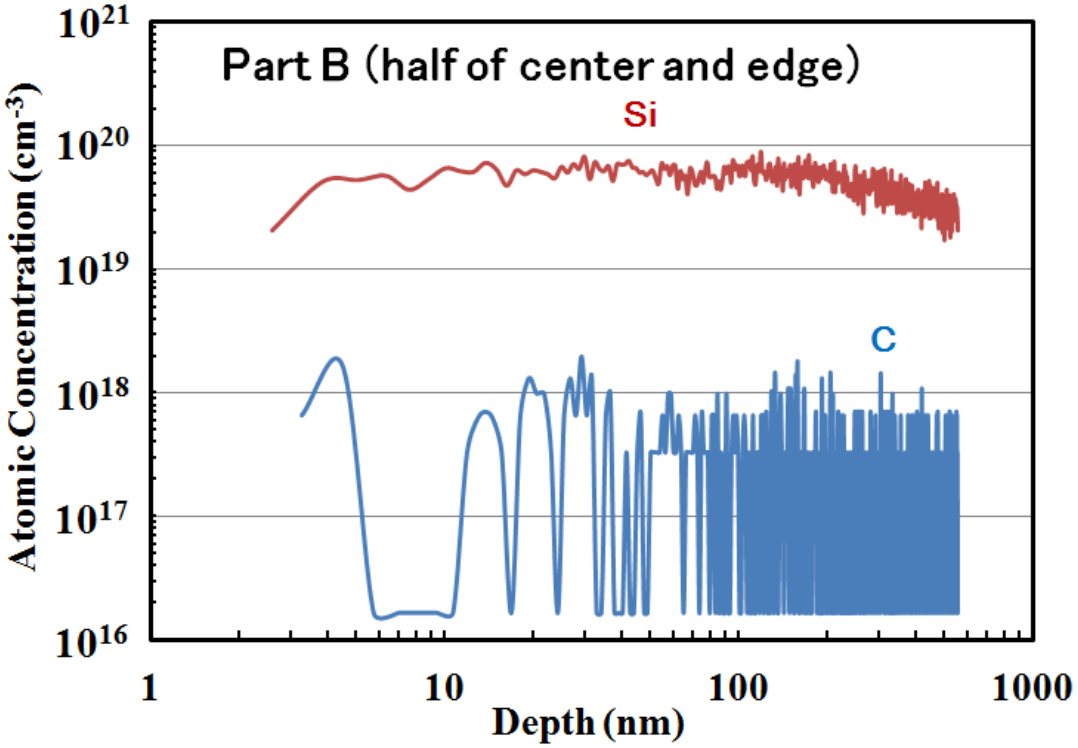

Fig. 9(b) Concentrations of C and Si in Part B of C-doped AlGaInN LED.

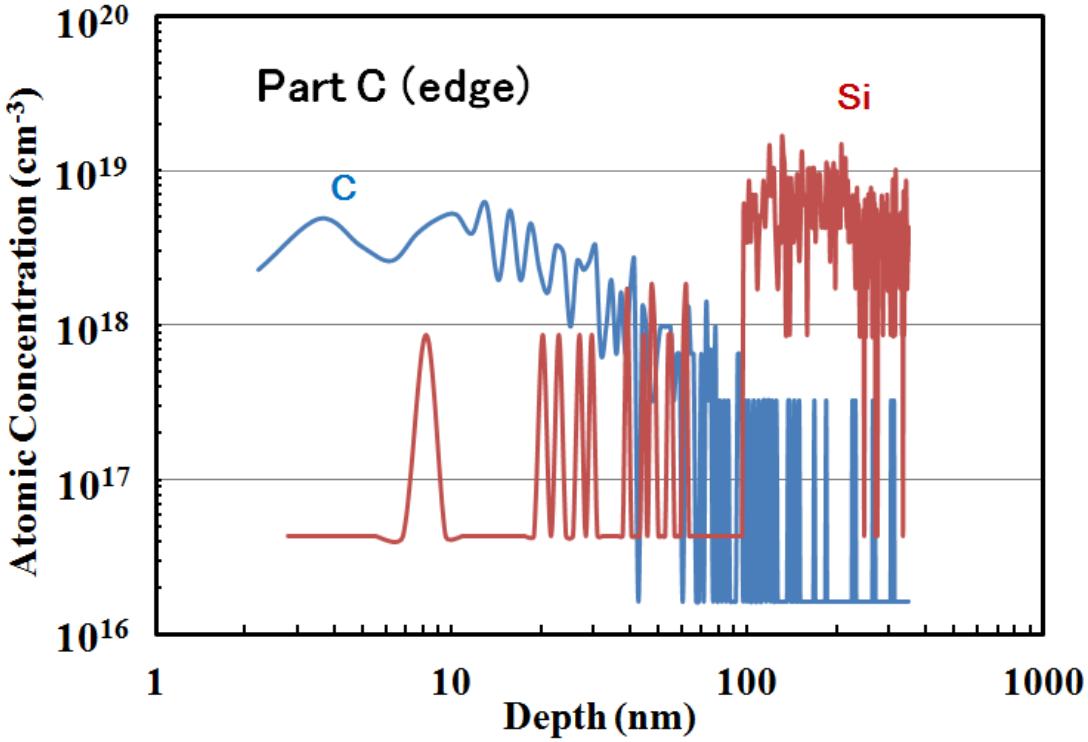

(c)

Fig.9(c) Concentrations of C and Si in Part C of C-doped AlGaInN LED.

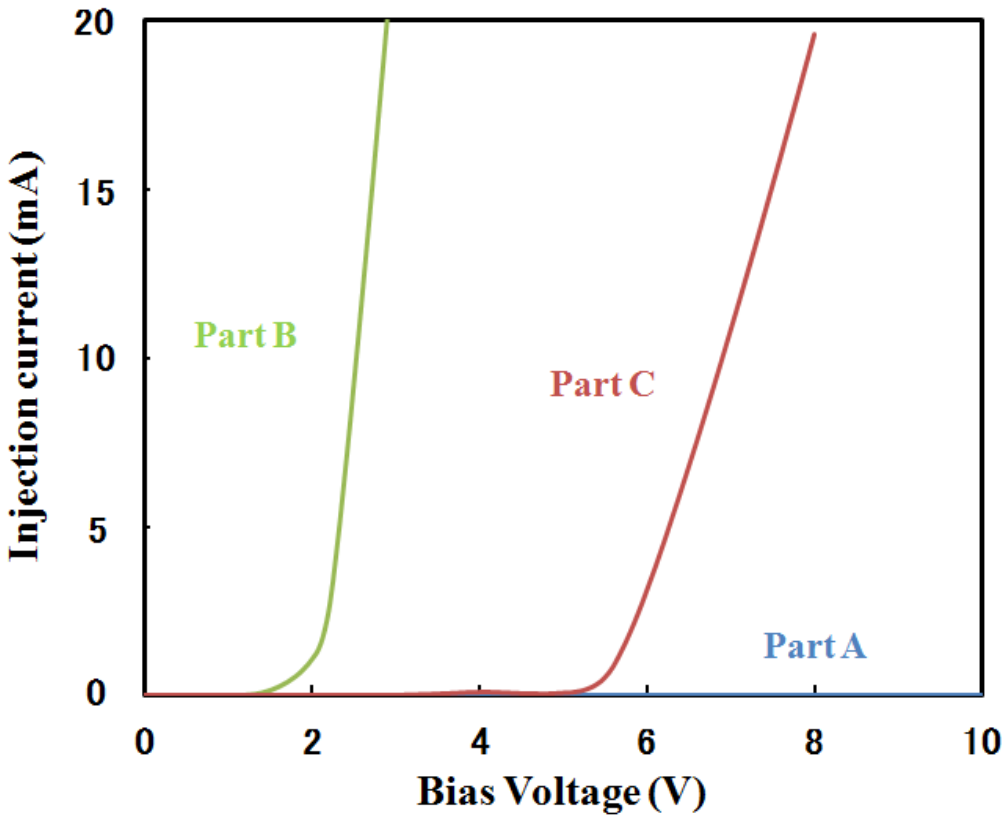

Fig.10 I–V measurements of C-doped AlGaInN based LED chips at a certain distance from Al_4C_3 sample in parts (A, B, C).

The measured I-V characteristics of C-doped AlGaInN LED along the distance from the black zone were shown in Fig. 10. Part A and B were not shown the characteristic of pn junction, but Part C (edge) was different. The bandgap energy of 3.1 eV was calculated by electroluminescence (EL) experiment, as shown in Fig. 12. Increase of conduction current was very small for part B. The voltage of part B was 2.6 V at the current of 10 mA. Also, conduction current of part A was large. This result corresponded to the Hall measurement of $Al_{0.20}Ga_{0.80}N$ and the SIMS analysis of the C-doped AlGaInN LED sample. As a result, only part C of C-doped AlGaInN LED showed the electric performance of C-doped AlGaInN LED.

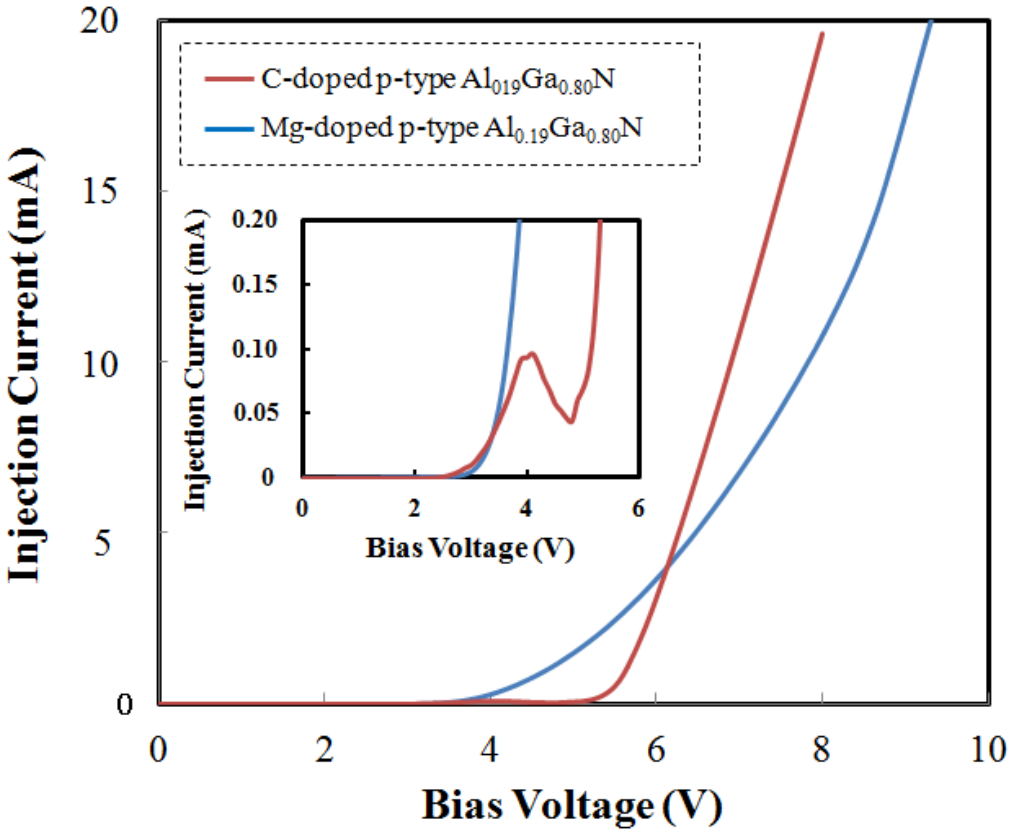

Fig.11 I–V characteristics of C- and Mg-doped AlGaInN LEDs.

I-V measurements of C- and Mg-doped AlGaInN LEDs are compared in Fig. 11. At a current of 10 mA, the voltages of 6.9 and 7.8 V were detected in C- and Mg-doped AlGaInN LED, respectively. It was clearly proven that AlGaN with a p-type conduction was formed by the Al_4C_3/Al_2O_3 (0001). Regardless of that, the current of C-doped LED had small peak from 4.1 to 4.8 V. It was shown in inset of Fig. 11. We think that the main reason is unwanted layer of n-type $Al_{0.20}Ga_{0.80}N$ formed on p-$Al_{0.20}Ga_{0.80}N$, as indicated in the Hall measurement section. In this case, a certain amount of voltage increase was supposed to be acceptable. The n-type layer formed on top of the p-type layer was covered with the depletion layer with the increase in voltage, and the current started to flow.

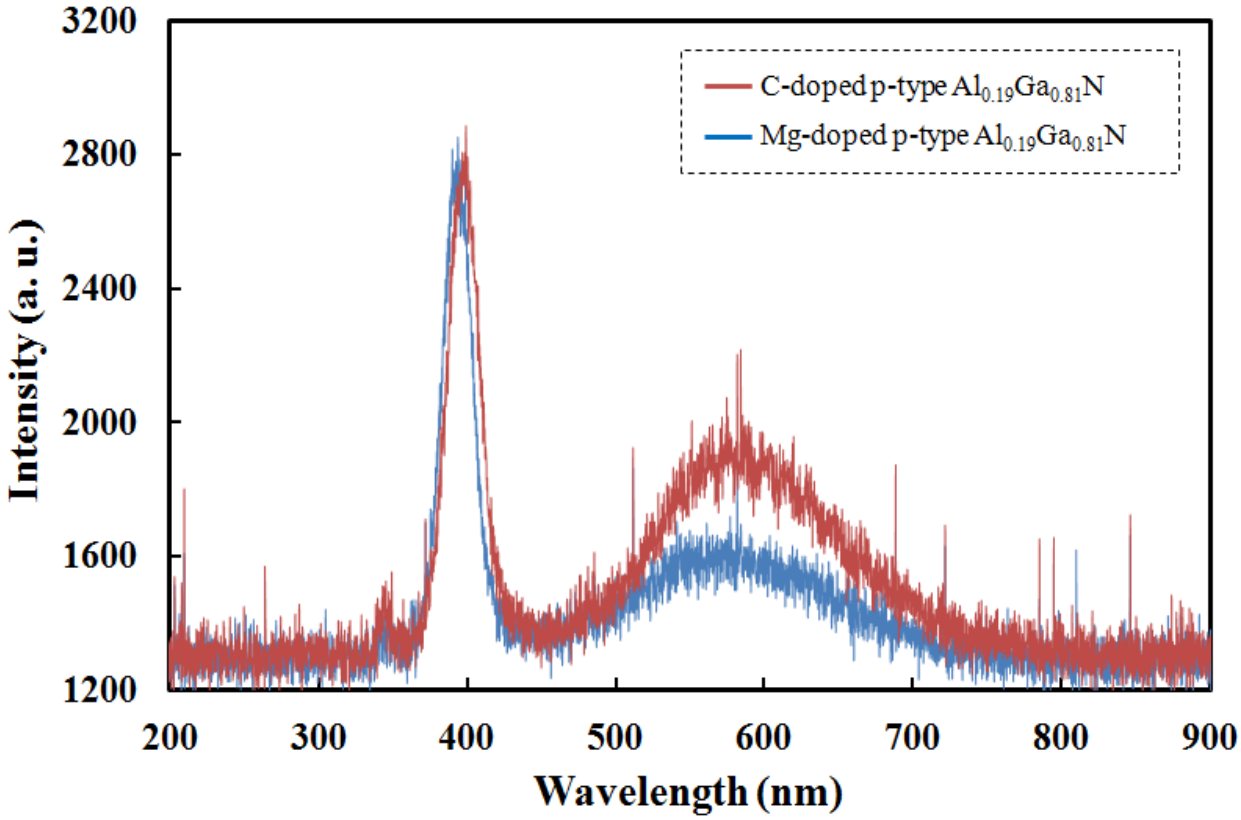

Fig.12 Electroluminescence peaks of C- and Mg-doped AlGaInN based LED chips.

The EL was measured as shown in Fig. 12. The C-doped AlGaInN LED fabricated by insertion of Al_4C_3 was showed almost same optical characteristic compare with Mg-doped LED. The peak wavelength and FWHM of the C and Mg- doped LED were at 395 and 390 nm, and about 30 nm, respectively.

4.4 Degradation in Al_4C_3

After growth, we analyzed Al_4C_3 (0001) layer grown by MOVPE. This sample shows darkish color. The scanning electron microscope (SEM) and energy disp ersive X-ray (EDX) spectroscopy analysis was performed to observe the surface and cross-section of Al_4C_3/Al_2O_3 (0001), as shown in Fig. 13(a) and (b). C was generally

detected. Si and Al were observed at the center. Also, Ga was detected.

According to Fig. 13(b), 1 μm Al_4C_3 layer was completely decomposed. The thickness of GaN grown on Al_4C_3/Al_2O_3 (0001) was thicker than GaN grown on Al_2O_3 (0001). This main reason is Al_2O_3 (0001) substrate thickness of 330 μm. We estimated that the growth speed of Al_4C_3/Al_2O_3 (0001) was 1.4 times higher than that of the Al_2O_3 (0001) substrate . Measured thickness of GaN grown on Al_4C_3/Al_2O_3 (0001) was 6.5 μm. The decomposition temperature of Al_4C_3 was 1000 ℃. Thus, Al_4C_3 was not detected in Fig. 13(b). Si atom was still observed in center of sample. It could be included in any part of the LED.

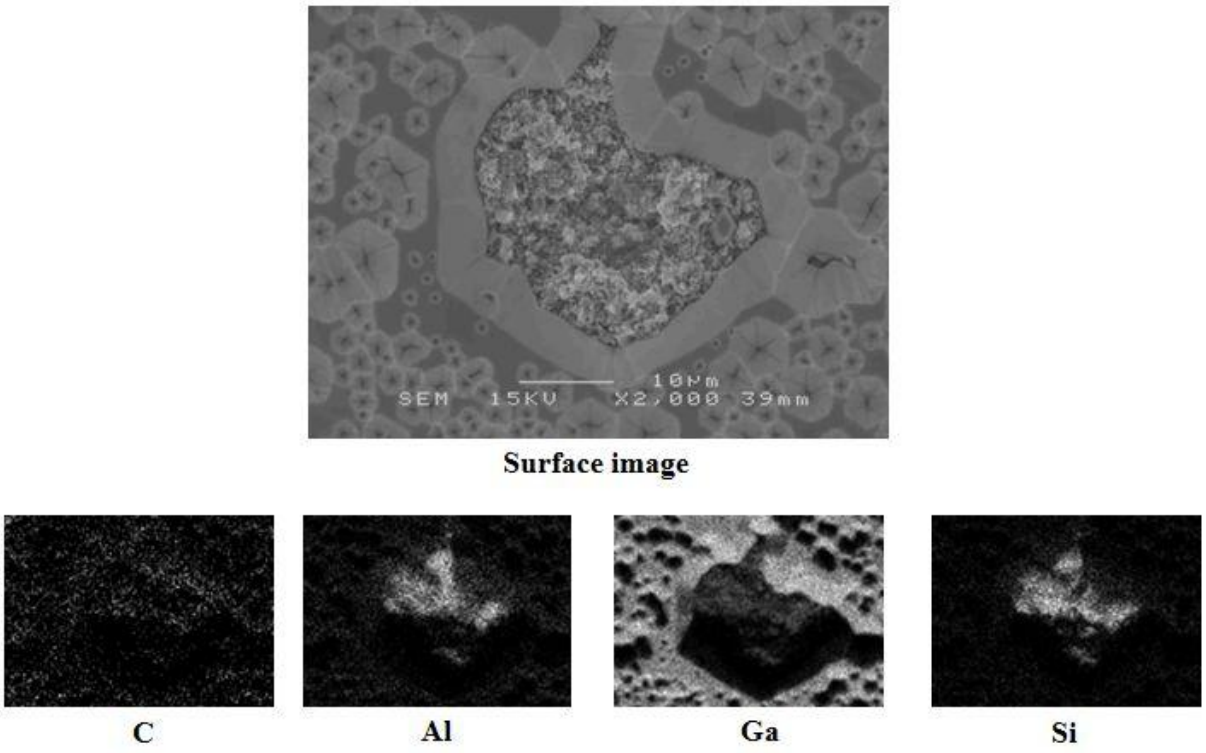

Fig.13(a) SEM and EDX images of surface Al_4C_3/Al_2O_3 (0001) used for C doping.

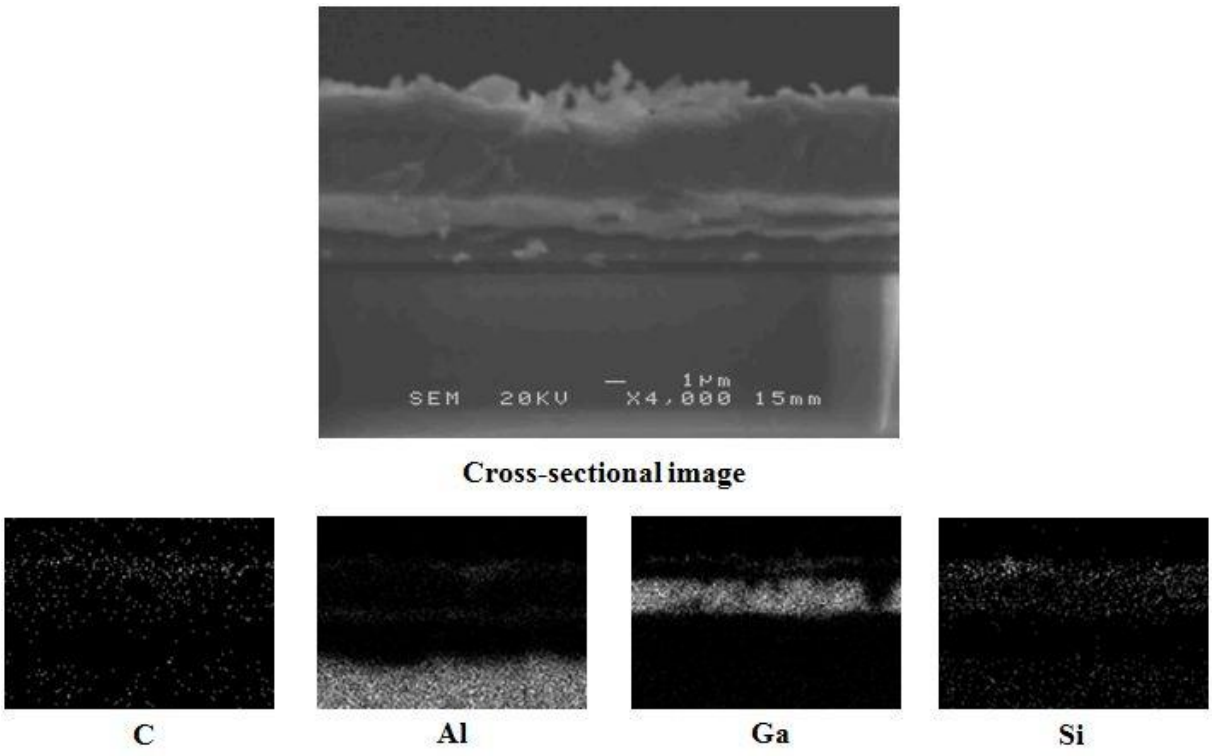

Fig.13(b) SEM and EDX images of cross-sectional Al_4C_3/Al_2O_3 (0001) used for C doping

4.5 Summary

C-doped AlGaInN LED was manufactured by the insertion of Al_4C_3/Al_2O_3 (0001). Manufactured LED device was observed at a certain distance from the inserted Al_4C_3. The voltage of the C-doped AlGaInN LED fabricated in Part C had 6.9 V at a current of 10 mA. The peak wavelength and FWHM of 395 nm and about 30 nm was measured by EL experiment. C-doped AlGaInN LED showed similar optical characteristics to a Mg-doped AlGaInN LED. By the insertion of Al_4C_3, p-type AlGaN with a C dopant was obtained in Part C. It is indicating that C was decomposed from Al_4C_3/Al_2O_3 (0001) and flowed into this Part C.

Reference

[1] F. Horie, Y. Naoi and S. Sakai: Ext. Abstr. (71st Summer Meet., 2010); Japan Society of Applied Physics and Related Societies, 16a-ZT-11.

[2] Y. Ohnishi, F. Horie and S. Sakai: Ext. Abstr. (59th Spring Meet., 2012); Japan Society of Applied Physics and Related Societies, 16p-F12-21.

[3] Y. Ohnishi, D. Kim, R. Oki and S. Sakai: Ext. Abstr. 6th Int. Conf. Si Epitaxy and Heterostrucrues, 2013, P2-17.

[4] D. Kim, F. Horie, Y. Onishi, Y. Naoi and S. Sakai: Ext. Abstr. 16th Int. Conf. Metal Organic Vapor Phase Epitaxy, 2012, TuP-71.

[5] F. Horie, Y. Ohnishi, Y. Naoi and S. Sakai: Ext. Abstr. (30th Summer Meet., 2011); Electronic Materials Symp., Th2-16.

[6] D. Kim, H. Lee, K. Yamazumi, Y. Naoi and S. Sakai: Jpn. J. Appl. Phys. **52** (2013) 08JG18.

[7] B. Arnaudov, T. Paskova, S. Evtimova, E. Valcheva, M. Heuken and B. Monemar: Phys. Rev. B **67** (2003) 045314.

CHAPTER 5

Conclusion

In this report, the experiments of diffusion and doping in AlGaN by Al_4C_3 were performed to obtain the p-type AlGaN. Also, the photo-induced current and its deterioration by oxidation in Al_4C_3/Al_2O_3 (0001) were reported.

In chapter 2, Al_4C_3 was grown by metalorganic chemical vapor deposition method. The growth rate of Al_4C_3 was increased with an increase in the growth temperature and trimethylaluminum (TMA) flow rate. On the contrary, the growth rate was decreased with a decrease in the IV/III ratio. Rhombohedral structure Al_4C_3 was not detected, but the hexagonal structure was shown to create. The yellowish surface of Al_4C_3 was changed to white color in air and it finally separated from the Al_2O_3 (0001), because of oxidation. The surface of Al_4C_3 stored in vacuum condition kept yellow color. PIC in Al_4C_3 increased with a decreased in the incident wavelength. The photo - induced current of Al_4C_3 was not related to the existence of a metal-semiconductor junction. This phenomenon was observed in absorption coefficient of Al_4C_3. Oxidation is main reason of the PIC deterioration . The PIC characteristic of Al_4C_3 can be applied for employment as a light sensor in equipment kept in vacuum or other gases which do not contain oxygen.

In chapter 3, the diffusion experiments of Al_4C_3 in AlGaN were shown. The characteristics of n- and p-conductivities were coexists in AlGaN with diffusion experiment. GaN and AlN without diffusion experiment were n-type and insulator in AlGaN with diffusion experiment. Also, these conductivities were not changed with diffusion experiment at 1000 ℃. Carbon diffusion length in AlGaN was significantly changed by Al amount in AlGaN. Also, the diffusion coefficient was showed same tendency. The diffusion length expected to Al_4C_3 was observed at the AlGaN surface. Al_xC_y binding energy was commonly detected in $Al_{0.45}Ga_{0.65}N$ and $Al_{0.65}Ga_{0.35}N$ with diffusion condition higher than 1000 ℃, excluding GaN sample with diffusion condition at 1000 ℃. It is

possible that Al_xC_y affect the formation mechanism of p-type AlGaN during diffusion experiment. Also, it was investigated that Al, C and O atoms of Al_xC_y were simultaneously diffused into the surface of AlGaN sample.

In chapter 4, Al_4C_3 was used as a p-type doping material for obtaining the p- type AlGaN. n- and p-type conductivities were different with the distance of Al_4C_3.Based on this research result, C-doped AlGaInN LED was fabricated by the insertion of Al_4C_3/Al_2O_3 (0001). Carbon concentration doped by Al_4C_3 in the growth procedure was different with the distance of Al_4C_3. Only edge of the grown wafer shows the electrical characteristic of AlGaInN-based LED. Maximum C ($p \geqq 10^{18}$ cm^{-3}) and Si ($n \geqq 10^{19}$ cm^{-3}) intensities were found at the edge and middle of grown wafer, respectively. The electroluminescence characteristic of C-doped AlGaInN with an InGaN/GaN multi quantum well (MQW) was showed almost the same as Mg-doped AlGaInN LED. The voltage of the C-doped AlGaInN LED was 6.9 V at 10 mA. The peak electroluminescence (EL) wavelengths and the full width at half-maximum (FWHM) were 395 nm and about 30 nm, respectively. Also, degraded Al_4C_3 during growth was investigated. C doping in AlGaN was made possible by the insertion of Al_4C_3. Also, it was clearly proven that u-$Al_{0.19}Ga_{0.81}N$ became p-$Al_{0.19}Ga_{0.81}N$.

A List of Related Paper by the Author

Papers

1. Fabrication of C-doped p-AlGaInN Light- Emitting Diodes by the Insertion of Al_4C_3, Dohyung Kim, Heesub Lee, Kazuya Yamazumi, Yoshiki Naoi and Shiro Sakai, Jpn. J. Appl. Phys, Vol. 52, 08JG18, August, 2013.

2. Photo-induced current and its degradation in Al_4C_3/Al_2O_3 (0001) grown by metalorganic chemical vapor deposition, Dohyung Kim, Yuya Onishi, Ryuji Oki and Shiro Sakai, Thin Solid Films, Vol. 557, p216-221, 2014.

Conferences

International Conferences

1. Fabrication of C-doped p-AlGaInN LED by the insertion of Al_4C_3, Dohyung Kim, Heesub Lee, Kazuya Yamazumi, Yoshiki Naoi and Shiro Sakai, International Workshop on Nitride Semiconductor 2012, TuP-OD-1, Sapporo, Oct, 2012.

2. Characteristics of Si and P-doped Al_4C_3 by Metalorganic Vapor Phase Epitaxy,Dohyung Kim, Fumiya Horie, Yuya Ohnishi, Yoshiki Naoi and Shiro Sakai, The 16th International Conference on Metal Organic Vapor Phase Epitaxy, TuP-71, Pusan, May, 2012.

Domestic Conferences

1. The Characteristic of Photo-induced current in Al_4C_3/Al_2O_3 (0001), Dohyung Kim, Yuya Onishi, Ryuji Oki and Shiro Sakai, The 74th Japan Society of Applied Physics, 17p-P9-2, Kyoto, Sept, 2013.

2. P-type conduction mechanism in Carbon-doped AlGaN, Dohyung Kim, Heesub Lee, Kazuya Yamazumi, Yoshiki Naoi and Shiro Sakai, The 60th Japan Society of Applied Physics and Related Societies, 28p-PA1-29, Kanagawa, Mar, 2013.

3. Diffusion of $Al_xGa_{1-x}N$ layer by Al_xC_y, Dohyung Kim, Heesub Lee, Kazuya Yamazumi, Yoshiki Naoi and Shiro Sakai, The 73rd Japan Society of Applied Physics and Related Societies, 12p-H9-15, Ehime, Sept, 2012.

Acknowledgment

I would like to express gratitude to people who have given me the favor during the re search at Japan. First of all, I would like to acknowledge Dr. Shiro Sakai who is famous scholar of Ultraviolet light-emitting diode field. He is my professor and competent researcher. I am also thanks for the help during the study at the University of Tokushima.

I wish to thank Professor Yoshiki Naoi, the member of my thesis committee, for useful assistance. He helped me second ion mass spectroscopy analysis of C-doped AlGaN samples.

I would like to acknowledge Professor Masao Nagase who is the member of my thesis committee. He gave me valuable comments and careful reviewing of the dissertation.

I would like to acknowledge Mr. Heesub Lee who is researcher of Seoulviosys co.Ltd. He helped my research activity.

I would like to acknowledge Miss Yunjung Choi, Mr. Shogo Wada, Mr. Fumiya Horie and Mr. Hiroyuki Hukuta. When I came to Tokushima first time, they gave me the useful advice and introduced to the experimental equipments.

I would like to acknowledge Mr. Kazuya Yamazumi. He was my tutor and studied the C-doped AlGaN. He helped my research activity.

Outside of that, I would like to express gratitude to tremendous kindness and cooperation of every doctoral and master course students in the Sakai laboratory.
Thank you so much!

I would like to acknowledge to Nitride Semiconductor. Co. Ltd. They gave the financial assistance to me. Especially, Mr. Suguru Nouda introduced the process condition of AlGaN based UV-LED chip.

I would like to acknowledge to KDDI foundation. They selected me as 2013 year international scholarship student. They made amusing memory in Japan in my last doctoral semester.

I would like to acknowledge my family. They encouraged me and gave their devotion. Without their support, I could not have finished my doctoral course.

Lastly, I would like to acknowledge many persons in University of Tokushima.